Bruno Cerqueira

# SoundForLife

Thesis submitted to the University of Coimbra in compliance with the requisites

for the degree of Master in Biomedical Engineering

September, 2016

· U C ·

UNIVERSIDADE DE COIMBRA

• U C •

FCTUC FACULDADE DE CIÊNCIAS
E TECNOLOGIA
UNIVERSIDADE DE COIMBRA

Bruno Miguel Dantas Cerqueira

# SoundForLife

*Dissertação apresentada à Universidade de Coimbra para cumprimento dos requisitos necessários à obtenção do grau de Mestre em Engenharia Biomédica*

*Thesis submitted to the University of Coimbra in compliance with the requirements for the degree of Master in Biomedical Engineering*

Supervisor:

Professor Paulo Fernando Pereira de Carvalho

Coimbra, 2016

This work was developed in collaboration with:

Centre for Informatics and Systems of the University of Coimbra

“Change is the law of life. And those who look only to the past or present are certain to miss the future.”

John F. Kennedy

# Abstract

Cardiovascular diseases are the leading cause of death around the world, representing a major problem regarding human health. Systolic time intervals (STI's) represent a possible solution to manage cardiovascular diseases. Being correlated to cardiac function, STI's represent a valuable resource in prognostic and diagnostic to access the heart condition and are a promising tool to deploy long-term follow-up cardiovascular disease management solutions. Heart sounds already proved to be a valuable approach to assess STI's [1].

In this thesis we propose new models for the Pre-Ejection Period (PEP) automatic extraction based in the heart sound (PCG), electrocardiogram(ECG) and Photoplethysmogram (PPG). PEP is estimated with a Bayesian approach, where the model proposed by Paiva et al. [1] is adapted. Heart sound processing is challenging as the optimal auscultation sites vary from individual to individual.

We also propose new models to extract PEP in a multi-channel approach where we use information from two different acquisition sites in order to exploit signal redundancy. The multi-channel models are based on the Bayesian approach from Paiva et al. [2], where the adaptation aims to improve the previous results by using a larger amount of information to assess PEP. The single-channel approach was evaluated on a group of 16 signal acquisitions from four healthy males, with four acquisitions for each individual. On the other hand, the multi-channel models were applied to signals from 8 healthy male subjects.

The results from the single-channel approach suggest that the inclusion of physiological properties extracted from PPG in the model reported by Paiva et al. [1] is a good procedure and the new approach can be applied to assess STI. On the other hand, the proposed multi-channel models do not improve the previous results. According to Paiva et al. [2], the multi-channel approach should be applied to assess STI's and our results suggest that it is better to use information only from the channel with the best performance.

# Resumo

As doenças cardiovasculares são a principal causa de morte em todo o mundo, representando um grande problema em relação à saúde humana. Os intervalos de tempo sistólicos (STI) representam uma possível solução para gerir este tipo de doenças. Sendo correlacionados com a função cardíaca, os STI representam um recurso valioso no prognóstico e diagnóstico sobre condição do coração, e são uma ferramenta promissora para implementar soluções de gestão de doenças cardiovasculares num acompanhamento a longo prazo. Os sons cardíacos já demonstraram ser uma abordagem útil para a avaliação dos STI [1].

Nesta tese propomos novos modelos que visam a extração automática do período de pré-ejeção (PEP) com base no som do coração (PCG), eletrocardiograma (ECG) e fotopletismograma (PPG). O valor de PEP é estimado com uma abordagem Bayesiana, onde o modelo proposto por Paiva et al. [1] é adaptado. O processamento de som do coração é um desafio pois os locais ideias para a auscultação variam de indivíduo para indivíduo.

Propomos também novos modelos para extrair o PEP partindo de um abordagem multi-canal, onde usamos a informação de dois locais de aquisição diferentes, com o intuito de explorar a redundância do sinal. Os modelos de multi-canal são baseados na abordagem Bayesiana reportada por Paiva et al. [2], onde realizamos uma adaptação com o objectivo de melhorar os resultados já obtidos, utilizando uma maior quantidade de informação para estimar o PEP. A abordagem realizada para um canal único foi avaliada num grupo de 16 aquisições de sinal, referentes a quartro voluntários saúdavéis do sexo masculino. Por outro lado, os modelos de multi-canal foram aplicados a sinais adquirides de 8 indivíduos do sexo masculino, também saudáveis.

Os resultados referentes à abordagem de canal único sugerem que a inclusão de propriedades fisiológicas extraídos a partir de PPG no modelo relatado de Paiva et al. [1] é um bom procedimento e que a nova abordagem pode ser aplicada para avaliar os STI. Por outro lado, os modelos de multi-canal propostos não melhoram os resultados anteriores. De acordo com Paiva et al. [2], a abordagem multi-canal deve ser aplicada para avaliar STI e os nossos resultados sugerem que é melhor usar as informações apenas a partir do canal com o melhor desempenho.

# Acknowledgments

I would like to express my sincere gratitude to my advisor Prof. Paulo Carvalho, for his daily readiness to help me during this thesis development, being as available and patient as possible. I want to emphasize the motivation he gave during all this process, and a special thanks for sharing his knowledge with me. I also would like to thank Prof. Rui Paiva for providing me with most of his works which served as substructure of this thesis. I am very grateful to Prof. Rui Paiva for his will to help me, always being available to clarify my doubts and help me with some problems. I thank to Ricardo Couceiro, for his help during the later stages of this thesis, providing me a data collection and some algorithms that were very helpful; also for always being ready to help me to understand them.

I want to thank to Centre for Informatics and Systems of the University of Coimbra (https://www.cisuc.uc.pt), and more specifically to clinical informatics cabinet, which always presented me good conditions of work, with all the resources necessary and a friendly environment as well.

To all my friends, for their daily motivation and support, for the good moments we spent together and for all the fun we had, serving as fuel to my daily work.

To my family, which always supported me in everything I needed, from the most logical to the most irrational moments.

Lastly, but not least, to my girlfriend, who despite the adversity has always been by my side, pushing me and supporting me every day. Her kindness, love and patience were the main reasons I kept motivated everyday even in the most difficult moments.

# Contents

# List of Figures

# List of Tables

# Abbreviations

| | |
|---|---|
| AV | **A**trioventricular **V**alves |
| AVC | **A**trioventricular **V**alves **C**losure |
| BCG | **B**allisto**c**ardio**g**ram |
| BPF | **B**andpass **F**iltered |
| CPW | **C**arotid **P**ulsate **W**aveform |
| CVD | **C**ardiovascular **D**isease |
| D-V | **D**orso-**V**entral |
| ECG | **E**lectro**c**ardio**g**ram |
| Echo | **Echo**cardiogram |
| HR | **H**eart **R**ate |
| HS | **H**eart **S**ound |
| H-F | **H**ead-to-**F**oot |
| ICG | **I**mpedance **C**ardio**g**ram |
| IA | **I**nstantaneous **A**mplitude |
| LSB | **L**eft **S**ternum **B**order |
| LVET | **L**eft **V**entricular **E**jection **T**ime |
| PCG | **P**hono**c**ardio**g**ram |
| PEP | **P**re-**E**jection **P**eriod |
| PPG | **P**hoto**p**lethysmo**g**ram |
| R-L | **R**ight-to-**L**eft |
| SC | **S**ignal **C**ontrast |
| SCG | **S**eismo**c**ardio**g**ram |
| SD | **S**tandard **D**eviation |
| STI | **S**ystolic **T**ime **I**nterval |
| STR | **S**ignal **t**o **N**oise |
| SV | **S**troke **V**olume |

# Chapter 1

# Introduction

## 1.1 Contextualization

Cardiovascular diseases (CVD's) are a major problem in human mortality, as it is the leading cause of death among Europeans and around the world. As Figure 1 demonstrates, in Europe, CVD is responsible for more than half of all deaths among women (51%), and a little less among men (42%). This represents around four million deaths per year. This huge numbers represent almost two time the number of deaths cause by cancer and shed light to how problematic CVD's are [3].

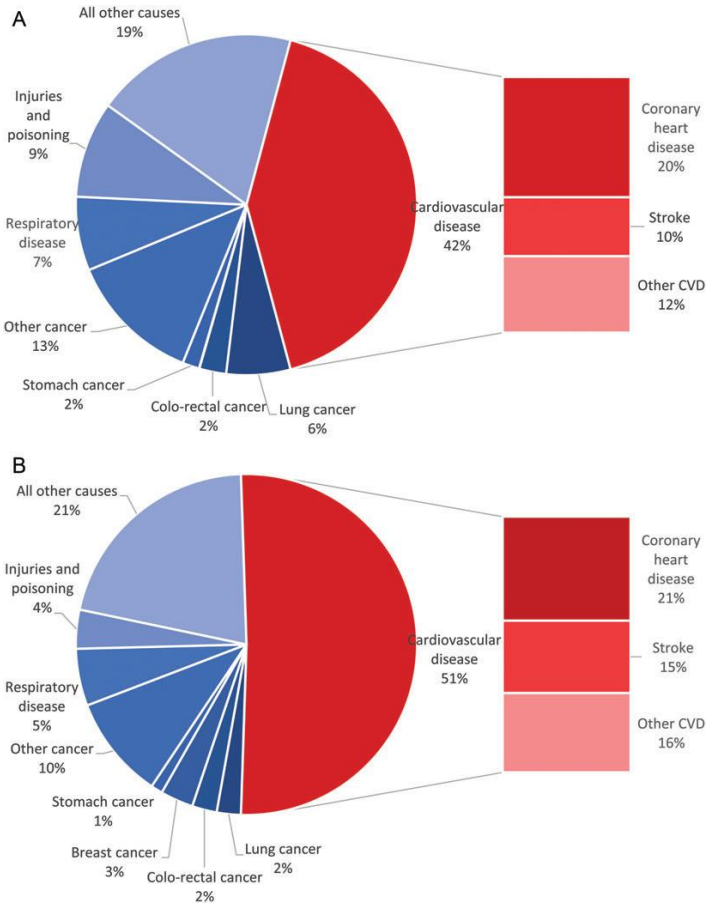


Figure 1- Proportion of all deaths due to major causes in Europe in 2014 among men (A) and women(B) [3].

CVD's are not only a health problem, but an economical one as well, being responsible for 10% of the total health care expenditure [4]. Therefore, developing a system capable of preventing and perform a good management of CVD's is a major goal for medicine in the current days. It is believed that the solution to this problem should follow a preventive long-term healthcare. This solution allows a reduction in costs by reducing hospital visits, and enable homecare. In this regard, long-term tele-monitoring is a promise tool to achieve this goal [1].

The main goal of this thesis is to study two systolic time intervals (STI's), PEP and left ventricular ejection time (LVET) exploring the heart sound. In this respect, there are two different theories behind the origin of the heart sound. The first one, is the valve theory, which claims that the sound is produced by the closure and opening of the heart valves. The second one is the cardiohemic theory, which states that the sound is produced by the entire cardiohemic system, i.e., by the vibration of structures that compose it, such as the heart cavities, the valves and the blood [4]. Heart Sound is divided in two main sounds, S1 and S2, related to systole and diastole, respectively. For this thesis, we assumed the first theory described in this paragraph.

Heart sound auscultation is a very important tool in medicine. The bio-signal resulting from this technique is usually acquired using a stethoscope. The analysis of this sound can provide important information regarding the condition of the heart [5]. Cardiac auscultation has been a powerful instrument for heart diagnosis, due to be a non-invasive and low-cost application.

A computed based auscultation provides new possibilities regarding health management. It is especially efficient in chronic disease management, being a low-cost and reliable solution, as required in long-term patient follow-up [1] [6].A computer based heart sound analysis provides an easier way to evaluate some cardiac disorders, such as valvar dysfunction and congestive heart failure [6].

Heart sound can be applied to extract systolic time intervals, such as PEP and LVET. STI's are highly correlated to fundamental cardiac functions, and have significant value in prognosis and diagnosis in heart failure condition [1]. Myocardial relaxation and contraction are controlled by intracellular recycling of calcium ions, and therefore, the timings of these cardiac events are directly related to the health of myocardial cells [7]. The blood flow in the systematic circulation is controlled by the left ventricle's function, acting as a pump. Therefore, the cardiac timings of this ventricle represent a major relevance in accessing the cardiac function. In the current days, there are some procedures

applied to obtain systolic and diastolic functions, such as echocardiography, which are performed in clinical facilities. As so, those procedures do not fulfill the requirements of this study goal, i.e., a daily application in home settings for a long-term patient follow-up. As it was reported in [7], the use of time intervals is a good solution for that case. The most important time intervals are PEP and LVET, regarding left ventricular systolic function.

## 1.2 Objectives

The objective of this thesis was to extract the Pre-ejection period (PEP) with a multi-channel approach. For this goal, phonocardiogram (PCG) and electrocardiogram(ECG) are used and echocardiogram represents as a gold standard for the values extracted. The first goal was to improve a Multi-Channel Audio-Based Estimation of the Pre-Ejection Period which was performed by Paiva et al. [2].

Initially, the established second goal of this thesis was to perform a segmentation of the second heart sound (S2), in order to study the correlation of the time interval between its main components and the cardiac function.

## 1.3 Organization

In order to maintain coherence throughout the thesis, the steps of this work are sequentially divided in 5 chapters. The first two chapters are devoted to establish a good background of the problem. As so, there's a brief review of heart's physiology, and a review of the technologies available to access systolic time intervals. To finish the introductory chapters, we provide a summary of the methods implemented and applied in the last years in order to develop a computer based extraction of STI's. The remaining chapters are devoted to explain the methods used in this thesis, as well as the results obtained.

**Chapter 1**

This is the current chapter. Here, a brief introduction of this thesis is presented, contemplating the motivation of our work and the objectives.

**Chapter 2**

This chapter starts with a brief review of the human heart physiology and anatomy. A large part of this chapter is devoted to an overview of the origins of heart sounds, and existing technologies used to study this sounds. The final part of this chapter is dedicated to a review of the works done in this area in the past years.

**Chapter 3**

The contributions of the thesis and the models already reported that we used are presented in this chapter. Every solution proposed to extract PEP is described in Chapter 3. In its first section, two Multi-channel audio-based approaches to extract PEP are described. The second part of this chapter described the method used in single-channel audio-based using PPG approaches.

**Chapter 4**

This chapter describes the results obtained for each method presented in chapter 3. We start with a review of the best performances across the models proposed, and finish with the analysis of the attempt made with changes in some parameters. At the end of each method results, a statistical analysis is performed in order to compare the results with the ones obtained by Paiva et. al.

**Chapter 5**

This chapter is composed of the main conclusions of the proposed methods, and the analysis of some possible challenges for the future.

# Chapter 2

# Background Concepts

## 2.1 Heart's Anatomy and Physiology

The heart is a part of the cardiovascular system. Its main function is to deliver blood rich in oxygen and nutrients to the body tissues through blood vessels. The heart is located in the thoracic cavity medial to the lungs and posterior to the sternum. It is involved in cardiac muscle, also called myocardium, and is divided in four chambers; the upper chambers are called the left and right atrium, and the lower chambers are called the left and right ventricles [8].

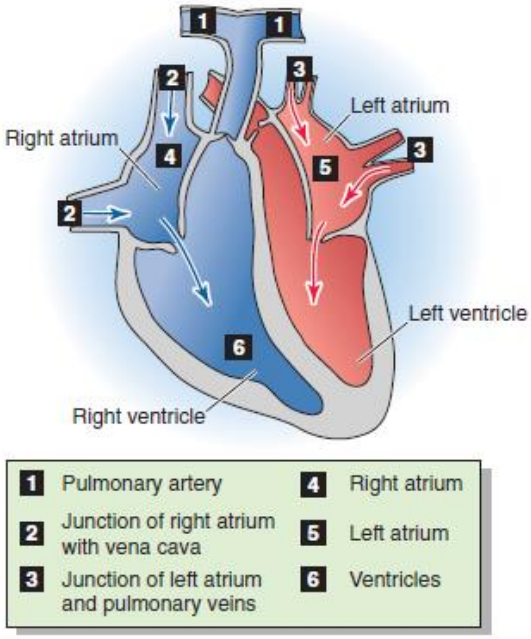


Figure 2- Anatomy of the human heart [8].

The human heart has four valves that regulate blood flow through the heart, two atrioventricular valves (respectively, the mitral valve and the tricuspid valve) and two semilunar valves (the pulmonary valve and the aortic valve) [8].

In a coordinated fashion, all valves open and close in order to enable or prevent blood from flowing, respectively. Tricuspid valve allows the communication between right atrium and right ventricle; on the other hand, pulmonary valve conducts right ventricle blood to the pulmonary artery in order to oxygenate it in the lungs. Mitral valve controls the blood flow from the left atrium into the left ventricle and aortic valve opens the way for blood to pass from the left ventricle into the aorta [8].

The pumping action of the heart is divided in two phases: diastole and systole. Diastole occurs when the semilunar valves close and the atrioventricular valves open. In this stage, the ventricles are relaxed and the heart is filled with blood. During systole the atrioventricular valves close and the semilunar valves open, the ventricles contract and eject blood from the heart [6] [8].

Systole is the interval between the first and the second heart sounds, lasting from the opening of the aortic valve to its closure. It is when the contraction of the heart happens. At this point, the atrioventricular valves snap, which results in the production of S1 [6] [9] .

Diastole is the term used to describe the relaxation of the heart. When the heart is in this state of relaxation the pressure within the heart is low. This is when blood is passively flowing through the atria and into the ventricles [6] [9].

In a normal human adult, there are two main heart sounds in each cardiac cycle, S1 and S2, induced by the closing of atrioventricular and semilunar valves, respectively. There are other cardiac sounds such as S3, S4 or even a great variety of murmurs [4] [6].

## 2.2 Phonocardiogram (PCG)

Phonocardiogram or PCG is a non-invasive clinical technique used to register heart sounds during a cardiac cycle [10]. In other words, PCG can be described as a digitized heart sound, being the interpretation of the sound waves produced by the heart during its function. Those sounds can be recorded in order to perform a detailed analysis and differentiate similar cardiac events that are difficult to discriminate by the human ear [10].

## 2.3 Electrocardiogram (ECG)

Based on electrical potential variations, ECG records the electrical activity generated by specialized heart cells over a determined amount of time [11]. A typical ECG consists of a P wave (atrial depolarization), a QRS complex (ventricular depolarization), and a T wave (ventricular repolarization) - Figure 4. The QRS complex is the main component of this signal, and it is commonly used to calculate heart rate in medical environments [12].

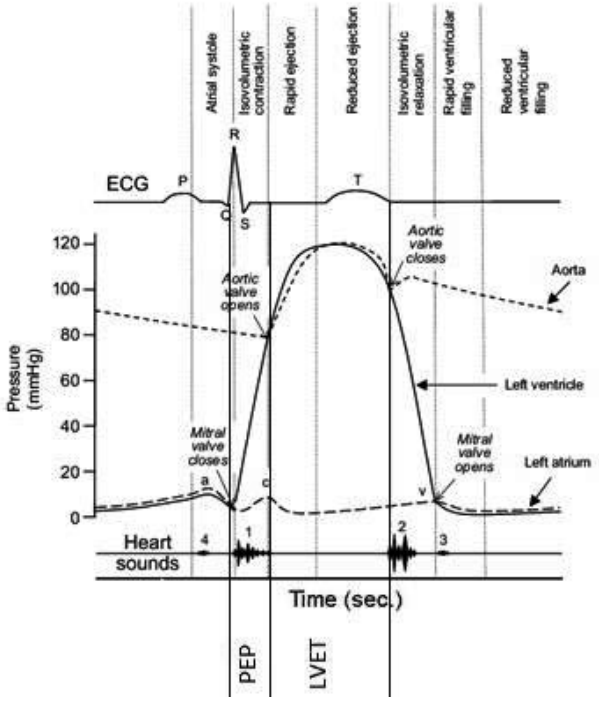


Figure 3 - Wiggers diagram describing the relationship between blood pressures and flows inside the left ventricle and corresponding events in the cardiac electrical and mechanical systems. Adapted from [13]

Figure 3 is very helpful to understand the relationship of heart sounds and a normal ECG with the heart cycle. It is also possible to correlate events such as heart valves closures and openings with the production of heart sounds.

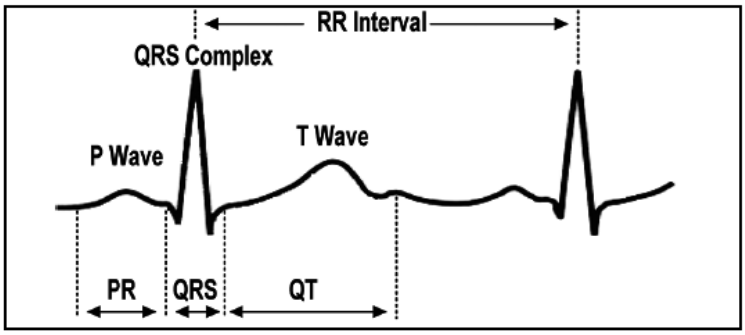


Figure 4 - Example of an ECG [14].

## 2.4 Photoplethysmogram (PPG)

Photoplethysmography is an optical technique, which typically operates using infrared light. It is very simple and low-cost and can be used to detect blood volume changes in the microvascular bed of tissue. The mechanism that generates PPG signals is composed by a complex interaction between the heart and connective vasculature [15] [16] [17].

The PPG waveform comprises a pulsatile (AC component) physiological waveform attributed to cardiac synchronous changes in the blood volume with each heartbeat which is called PPG signal. It is superimposed on a slowly varying (DC component) baseline with various lower frequency components attributed to respiration, sympathetic nervous system activity and thermoregulation. The pulsatile AC PPG waveform is named PPG signal [15] [16] [17].

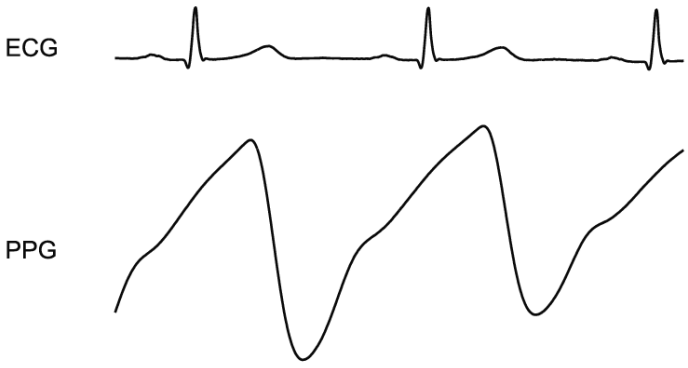


Figure 5- The pulsatile (AC) component of the PPG signal and corresponding electrocardiogram (ECG) [15].

## 2.5 Heart Sound and Auscultation

As it was mentioned previously, heart sounds are measured via phonocardiography, which is the process of listening the sound via stethoscope. There are four different heart sounds that can be listened, apart from murmurs [18] .

The first heart sound or S1 occurs when leaflets of mitral and tricuspid valves close in a coordinated way [8]. Therefore, S1 comprises two different components, M1 and T1. M1, which usually comes first than T1, results from mitral valve closure. On the other hand, T1 is produced when tricuspid valve closes. Due to higher pressures on the left side of the heart, M1 component is louder than T1 [4] [6] .

The closure of aortic and pulmonary valves generates the second heart sound or S2 [8]. Like S1, S2 is also consisted by two components termed A2 and P2. A2 is considered the main component of S2 and is resulted from aortic valve closure. In turn, P2 occurs when the pulmonary valve closes. Usually A2 is louder than P2, for the same reason as M1 is louder than T1 [4] [6].

The third heart sound or S3 is an extra sound that could be heard in early diastole during the ventricular rapid filling phase of the heart cycle [8]. S3 is also known as protodiastolic gallop or ventricular gallop as the sequence S1-S2-S3 sounds like a galloping horse. S3 might be present in normal children and teenagers as a result of a limited ventricular distensibility due to lack of cardiovascular system maturity [8]. Although S3 could be audible in an adult, its presence in those cases may be indicative of cardiac pathology and heart failure [8]; the volume overload in the ventricles difficult its recoiling process and forces them to provide extra recoiling power. The marked recoil results in an audible S3 [8]. Repetition of this situation will end in a dilated ventricle [6] [19].

The fourth heart sound or S4 is an extra sound that occurs during the atrial filling phase of ventricular diastole and only can be heard in pathological situations [8]. When there is a pathological situation that combines a strong atrial contraction with a non-compliant left ventricle results in S4. S4 is heard due to blood striking the ventricle [8] [20]. S4 is also classified as a gallop sound as the sequence S4-S1-S2 resemble a galloping horse. Therefore, S4 is known as presystolic gallop or atrial gallop [8].

Finally, there are the heart murmurs, or abnormal heart sounds, which are mainly associated with turbulence in blood flow. Murmurs differ between themselves, and are classified by their loudness, frequency, timing, quality and shape [8].

As it was mentioned previously, the main goal of this thesis is to extract STI's, more precisely PEP. PEP and LVET relevance and its relationship with the heart's function will be explored later in this chapter.

## 2.6 Heart Sound Segmentation

As it was mentioned previously, noninvasive methods such as phonocardiogram (PCG) and electrocardiogram (ECG) are really useful in studying heart's condition. In auscultation process, the listener has to analyze the sound components and synthesize the heard features. The analysis is very dependent on listener skill and experience, and as so, computerized analysis is vital to help cardiologists in this field. In order to do any computerized analysis of heart sound, the former need to be segmented into its components to be possible to analyze those components separately [21] [22].

Segmentation can be divided in two main different approaches. It can either be done with help of an auxiliary signal, or it can be done with the heart sound signal alone. In the first scenario, the auxiliary signal is usually a signal that requires less processing steps, and it is used to extract markers coinciding the main heart sounds. This seems to be a good procedure to do when we are trying to segment heart sound. However, adding a second signal implies adding hardware complexity and decreasing the user friendliness. As so, the segmentation of heart sound using no auxiliary signal is the ideal scenario. We can divide this type of approach in two components: unsupervised approaches and supervised approaches. Despite both approaches require a training dataset, the major difference between these two is that in the last one a typical pattern recognition approach is applied [6] .

In this thesis we study the segmentation of the first heart sound in aortic (A1) and pulmonary (P1) components.

## 2.7 Systolic Time Intervals

Many studies proved that heart sounds can be applied to measure the systolic time intervals we were interested in, pre-ejection period and left ventricle ejection time.

Systolic time intervals are highly correlated to fundamental cardiac functions. A large number of studies proved that these measurements have significant diagnostic and prognostic value in heart failure condition. The most adequate application is for long-term patient follow-up and disease management [1].

Pre-ejection period, or PEP, is the time interval between the start of ventricular depolarization and the moment when aortic valve opens. PEP's main utility is reflecting the condition of the left ventricular function, and it allows to see changes in myocardial contractility, left ventricular end-diastolic volume and aortic diastolic pressure [23] [24] .PEP is also very useful as a non-invasive beat-to-beat surrogate to estimate the blood pressure. To take a closer look on PEP's main role, we can find a review in Muehlsteff et al. [25].

Left ventricular ejection time, or LVET, is the time interval between the opening of the aortic valve and its closure. Studies reveal that LVET is related to cardiac output [26] and to contractility [24], thus we can say LVET is a measure of cardiac function.

The sum of PEP and LVET is the total time the heart spends in systole (ejection) as compared to diastole (filling) and is an important parameter for monitoring of patients with heart disorders [27].

The STI's can change according to heart rate, preload, afterload and myocardial inotropic state [28]. These four determinants do not influence every systolic time interval in the same way, in fact, not every determinant influence every STI. By definition, preload is the amount of stretch in the left ventricle at the end of diastole [29]. The contraction of myocardial cells is directly related with the amount of stretch they are under, therefore, the greater the stretch, the greater will be the force of contraction [29]. On the other hand, afterload represents the force that heart must overcome to open the aortic valve and eject blood into the systemic circulation [29]. Myocardial inotropic state refers to myocardium contractility, i.e., the term inotropy refers to a measurement of the increase of myocardium contractility [29]. The greater the contractility of the heart, the greater will be the cardiac output [29].

PEP increases inversely with preload and stroke volume (SV) and directly with afterload. Thus, a decrease in preload will cause an increase in PEP value and a decrease will shorten PEP. On the other hand, a rise on afterload is translated by an increase in PEP value; a decrease will produce a lower value of PEP. Regarding myocardial contractility, the presence of positive inotropic agents leads to an increase of inotropy and consequently a stronger myocardial contractility, which reduce the time of PEP [28]. The opposite is also true, i.e., PEP interval is elongated by the presence of negative inotropic agents. Regarding LVET, this systolic time interval has an opposite behavior with changes in preload and stroke volume. Thus, an increase in preload and SV will increase LVET and a decrease will shorten this interval. Afterload can only influence LVET to grow, since any change in afterload, no matter its nature, can cause an increase in LVET. On the other hand, inotropic agents can affect LVET in order to decrease it, no matter their nature [28]. STI's in general vary inversely with heart rate [30]. Therefore, corrections related to differences in heart rate must be done in order to properly interpreter STI's deviations [30]. To this end, regression equations for each STI were derived, and used to derive STI indices. Each index is calculated as the sum of the extracted interval with heart rate multiplied by slope of the regression equation [30]. These indexes are useful to extract a quantitative measure of the degree of deviation between the calculated STI and the one expected as normal. There is no agreement in what are the most efficient regression equations, being the most applied the ones derived by Weissler et al. [31].

PEP interval is usually around 90 ms [32], leading to an index of 131 in females and 133 in males when the heart rate is added as a factor [31]. LVET usually last around 300 ms [32], with an index value around 413 ms for women and 418 ms for men when the heart rate in taken into account [31].

As far as PEP and LVET are concerned, usually a short PEP and long LVET represent a healthy heart [33]. On the other side, a myocardial dysfunction extends PEP and shortens LVET [34]. There are many more cardiac dysfunctions that can be identified purely based on systolic time intervals, reported in [35].

## 2.8 Relevant Studies using Systolic Time Intervals

This field is not an unexplored area. Some attempts to extract systolic time intervals and even correlating them to clinical assessment of heart condition have been done in the last years.

However, it seems that there is significant space to improve like everything in science. Like it was mentioned previously, we find Systolic time intervals an area of vast interest due to its correlation with cardiac function.

Currently, there are many technologies available to access STI's. Carvalho et al. [34] performed an evaluation contemplating most of this technologies, that will be described forward. Some of this technologies were already described previously, such as electrocardiogram (ECG), phonocardiogram (PCG) and photoplethysmogram (PPG). Those alongside impedance cardiogram (ICG), are the most used in this area of interest. In the past years, some projects using echocardiogram as a gold standard were reported, and they will be described forward in this section. Apart from these, ballistocardiogram (BCG) and seismocardiogram (SCG) can also be used to assess STI's, as in [36].

### 2.8.1 Relevant Studies using Systolic Time Intervals: Part I

Hongyan Luo and Zhigang Wang [37] developed methods of automatic analysis for systolic time intervals in 2000. They applied a slope method for detecting characteristic points of ECG and carotid pulsate wave (CPW), and an algorithm based on wavelet transform is implemented for analysis of PCG [37].

They used a slope method to detect R-peaks in ECG, and according to their results it is possible to see that R-peaks are correlated with the slopes.

The carotid pulsate waveform (CPW) consists of three waves and a notch. Since the ECG signal and CPW signal were recorded simultaneously, each complete cycle of CPW is located between two R-wave peaks. The CPW peak is the maximum amplitude point meeting the condition of being between the R-peaks. The start is the nearest point from the baseline [37].

Applying the slope method to CPW, it is possible to see that the characteristics of dicrotic notch are more outstanding [37].

To detect PCG signal characteristic points they used a wavelet transform method. The binary wavelet transform of the digital signal was performed by Mallat algorithm [37].

As described in [37], wavelet transforms in different scales can be used to see components with different frequency. As so, they were able to extract features of S1 and S2, as well as their location, using the scale 2. S1 was identified as the maximum point of the wavelet transform PCG signal, meeting the requirements of being between R-wave peak and the peak of CPW. The maximum value between the peak of PCG wave and the dicrotic notch of CPW was considered to be S2 [37].

Based on the total 100 cases they studied and on scientific literatures, they developed a criterion of classification for cardiac function, shown in Table 1. It should be taken in consideration that Heart rate (HR) has an influence in the values of PEP and LVET as described previously, so the following results are obtained considering a normal value for heart rate between 60 and 100 bpm's [37].

Table 1- Criterion of classification for cardiac function [37].

| Parameter / Level | LVET (ms) | PEP (ms) | PEP/LVET |
|---|---|---|---|
| **Normal** | ≥300 | ≤90 | ≤0.30 |
| **Approximately normal** | 281~299 | 91~105 | 0.31~0.34 |
| **Lightly weaken** | 271~289 | 106~120 | 0.35~0.38 |
| **Weaken** | 251~269 | 121~140 | 0.39~0.49 |
| **Obviously weaken** | ≤250 | ≥141 | ≥0.50 |

Table 2- A comparison study between the new system and an existing system accuracy's [37].

| Points / System | Q wave start | R-peak start | CPW start | CPW peak | CPW dicrotic notch | S1 | S2 |
|---|---|---|---|---|---|---|---|
| **New System** | 92.5% | 97.5% | 92.5% | 97.5% | 92.5% | 95% | 95% |
| **Existing System** | 87.5% | 90% | 85% | 87.5% | 75% | 80% | 80% |

The results provided by the authors were very positive. They show that the new system can obtain higher accuracy in every point, with a special increase in detection of dicrotic notch, the first and the second heart sound [37].

### 2.8.2 Relevant Studies using Systolic Time Intervals: Part II

Abdul Q. Javaid et al. [36] [38] also has some relevant studies about measurement of systolic time intervals. There are two remarkable studies that he leads about this field, which will be explored in this section.

In 2015 Abdul Q. Javaid et al. [38] worked on a way to estimate systolic time intervals using head-to-foot and dorso-ventral components of sternal acceleration signals. Acknowledging systolic time intervals is a major interest for monitoring cardiac functions, Abdul Q. Javaid thought that continuous measurement of cardiac time intervals throughout daily living had a special interest to this goal. The objective of his study was to measure PEP and LVET with wearable sensors based on ballistocardiogram (BCG) and seismocardiogram (SCG) measures. They present methods for estimating the systolic time intervals from a single three-axis accelerometer placed at the sternum. Also, they show that the method is insensitive to certain postural changes [38].

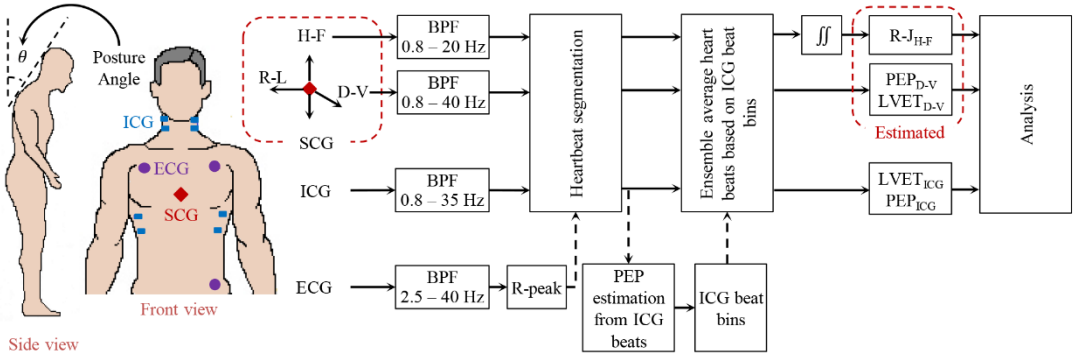


Figure 6- Block diagram of the setup. The subjects were asked to stand in three different postures while an accelerometer, ECG and ICG electrodes were placed on the body locations specified by the front view. The data collected from all sensors was bandpass filtered (BPF) followed by subsequent processing and analysis [38].

PEP and LVET were extracted from impedance cardiogram (ICG), from the dorso-ventral components of the SCG signal and from the Head-to-foot components of the SCG signal. A study of the correlation between these extractions was made afterwards [38].

Using STI's extracted from ICG as a gold standard, the correlation results suggest that for PEP estimation, the double integrated head-to-foot component of the SCG waveform (very alike BCG waveform) is better than the dorso-ventral component. At the same time, the dorso-ventral component provides a robust estimate of LVET [38].

In 2016 Abdul Q. Javaid et al. [36] published other study about approximately the same theme. This study is focused on estimating PEP and LVET during walking based on ballistocardiogram (BCG). They demonstrated a good correlation between PEP from ICG and the BCG features, and also LVET estimated from both ways [36].

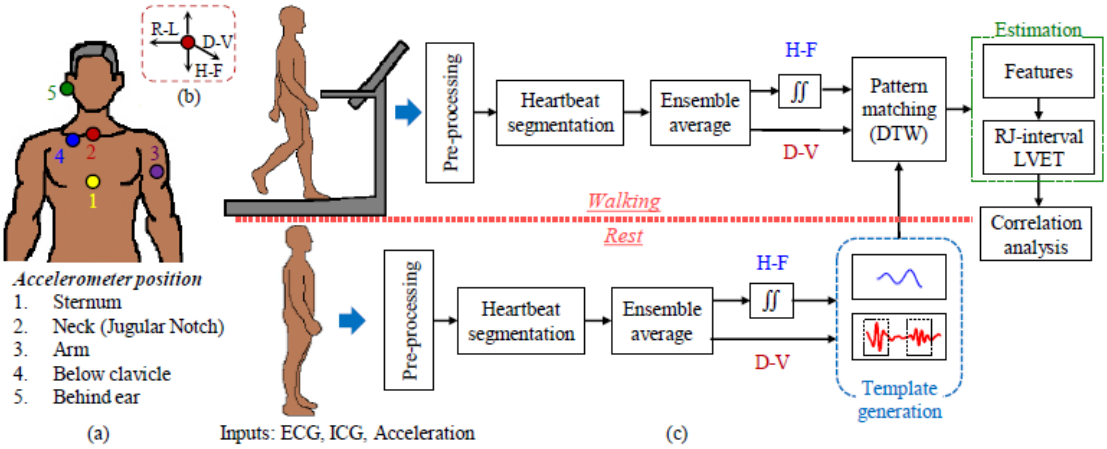


Figure 7- (a) Position of accelerometers on the body. (b) The head-to-foot (H-F), dorso-ventral (D-V) and right-to-left (R-L) axis of the accelerometer. (c) Block diagram of the setup. Data were collected in resting and walking states [36].

To calculate LVET they used data from D-V axis and from the neck and sternum accelerometers. On the other hand, the H-F data from all accelerometers were used to estimate the RJ-intervals. They employed data fusion to improve the correlation between the accelerometer and ICG estimated parameters during walking [36].

The results suggest that this method combined with fusion of estimates from more than one sensor can provide an assessment of cardiac health during walking [36].

### 2.8.3 Relevant Studies using Systolic Time Intervals: Part III

University of Coimbra, more specifically Centre for Informatics and Systems of the University of Coimbra (CISUC), has been working on systolic time intervals detection for the last years. The following paragraphs describe a further study based on the ones that were already performed by this institution. We find important to make a review about what has been done in the past, and what are the root of this thesis.

In 2009 Carvalho et al. [39] investigated the feasibility of measuring opening and closing moments of the aortic valve, using heart sound. These moments are very important, since they are crucial to define both PEP and LVET. Heart sound was used to extract several features with the goal of define these STI's. A secondary goal of their study was to measure the accuracy in using heart sounds to measure aortic valve opening and closing times [39].

This study was performed with 17 volunteers, providing both heart sounds and echocardiography (echo). A synchronous ECG with each of the above signals was also acquired and served as a reference signal for co-registration [39].

Echocardiography's were used to take annotations of the opening and closing instants of aortic valve, under the supervision of an experienced clinical expert in this area. Regarding the heart sound, the annotations were performed by them, without echo reference, using features from heart sound and ECG signals [39].

Table 3- PEP identification results from Carvalho et al. [39].

| Signal | Average ± SD (ms) | Range |
|---|---|---|
| **Echo** | 54.04 ± 18.22 | [22.02, 109,97] |
| **HS** | 52 ± 17.13 | [27.77, 106,58] |
| **Error*** | 5.81 ± 4.91 | - |
| ***\|$PEP_{HS}$-$PEP_{Echo}$\|** | | |

Table 4- LVET identification results from Carvalho et al. [39]

| Signal | Average±SD (ms) | Range |
|---|---|---|
| **Echo** | 266.01±27.67 | [180.54, 328.95] |
| **HS** | 255.13±25.41 | [176.85, 326.05] |
| **Error*** | 14.76±10.94 | - |
| ***\|$LVET_{HS}$-$LVET_{Echo}$\|** | | |

Table 5- AVC identification results from Carvalho et al. [39].

| Signal | Average ± SD (ms) | Range |
|---|---|---|
| **Echo** | 320.05 ± 26.46 | [222.63, 328.95] |
| **HS** | 307.95 ± 22.84 | [250.49, 362.98] |
| **Error*** | -12.10 ± 14.71 | - |
| ***$AVC_{HS}$-$AVC_{Echo}$, where AVC stands for Aortic Valve Closure** | | |

The achieved results are shown in Table 3, Table 4 and Table 5, suggesting that is possible to identify systolic time intervals from heart sound with accuracy. The errors ae significantly low and according to their reports the correlation value between the calculated values and the ones from echocardiography was high.

In 2010 the study of systolic time intervals was carried further, and Carvalho et al. [34] performed a study using the echocardiographic gold standard synchronized with impedance cardiography (ICG), phonocardiography (PCG) and photoplethysmography (PPG).

Regarding ICG, they present results for several definitions for ICG characteristic points of aortic valve events. These results reported for ICG are obtained with the algorithms reported in [40] , [41] and measurements achieved by Niccomo device from Medis (abbreviations ICGZC, ICGOnu ICGCarvalho and ICGNiccomo, respectively).

Phonocardiography results were obtained applying a modified version of the algorithm reported in [42].

PPG signal was used to estimate LVET, since there is no known solution to extract PEP. The PPG waveform analysis is based in an approach reported in [43].

Table 6 - Summary of results for PEP from Carvalho et al. [39] ρ- correlation with echocardiography.

| **Parameter** | **Est. Error (msec.) (average ± SD)** | **Abs. Est. Error (msec.) (average ± SD)** | $\rho$ |
|---|---|---|---|
| **$ICG_{ZC}$** | -7.2 ± 28.6 | 23.9 ± 17.2 | 0.75 |
| **$ICG_{Onu}$** | 16.5 ± 16.7 | 19.9 ± 13.4 | 0.68 |
| **$ICG_{Carvalho}$** | 5.8 ± 14.0 | 12.4 ± 8.7 | 0.54 |
| **$ICG_{Niccomo}$** | 9.8 ± 21.4 | 19.3 ± 13.4 | 0.58 |
| **PCG** | 0.7 ± 11.0 | 9.0 ± 6.4 | 0.54 |

Table 7 - Summary of results for LVET. ρ - correlation with echocardiography [39].

| **Parameter** | **Est. Error (msec.) (average ± SD)** | **Abs. Est. Error (msec.) (average ± SD)** | $\rho$ |
|---|---|---|---|
| **$ICG_{Onu}$** | 1.8 ± 46.2 | 39.1 ± 24.5 | 0.19 |
| **$ICG_{Carvalho}$** | -23.6 ± 31.1 | 29.9 ± 25.1 | 0.36 |
| **$ICG_{Niccomo}$** | 51.2 ± 45.8 | 54.3 ± 42.1 | 0.27 |
| **PCG** | -9.9 ± 16.3 | 14.4 ± 12.4 | 0.80 |
| **PPG*** | 0.9 ± 14.2 | 11.5 ± 8.95 | 0.77 |
| *** Only apllied over a subset of 112 beats where PPG was available.** | | | |

The best overall performance was achieved using heart sound to measure systolic time intervals. The results suggest that PCG and PPG have the potential to build monitoring systems for long-term cardiac function follow-up, despite the correlation value not being very high (calculated using Matlab) [34].

The previous study has been carried further by Paiva et al. [1] in 2012. After the results from [34] this study focused in investigating the feasibility of using heart sound to extract PEP and LVET. The paper [1] was the basis for this thesis, i.e. the starting point of this work was to find ways to improve the accuracy of the model from [1] to extract systolic time intervals. The methods used by Paiva et al. [1] will be described in the forthcoming section. The hypothesis of heart sound containing important markers that enable the detection of aortic valve opening and closing is the basis of Paiva´s [1] study and this thesis. To evaluate the accuracy of this methods, an echocardiography was used as a gold standard [1].

PEP was estimated following a Bayesian approach where the main features were the instantaneous amplitude of heart sound, and the delay between aortic valve opening and atrioventricular valve closure [1]. To extract LVET, sound segmentation was performed and the segments nearest the T-wave were taken as S2 candidates [1].

The results suggest that heart sound is a possible option to detect systolic time intervals, being the biggest motivation of this thesis [1].

# Chapter 3

# Materials and Methods

In this chapter the methods applied and the data collections used will be described. The first subsection is dedicated to understand the algorithms developed by Paiva et al., reported in [2] and [1] , which are the basis of this thesis. This project starts from creating two methods for a two-channel audio-based estimation of PEP, where the main objective is to use information from the worst channel to extract PEP from the best channel, in order to improve the results obtained by Paiva et al. The best channel selection is performed according to the algorithm reported in [2]. For the sake of completeness, methods reported in [1] and [2] will be described in the next subsections. The second stage of this project consists in the description of two models used to perform a single-channel audio-based estimation of PEP using PPG. The model is based in the algorithm reported in Paiva et al. [1], where PPG is added to extract LVET and consequently a PEP value for each beat, which will serve as an additional parameter to assess PEP from heart sound. Every method used will be described in the following sections in order to understand how the models created work.

## 3.1 Multi-channel Audio-based Estimation of PEP

### 3.1.1 Overview

This section describes each one of the steps taken in the approach studied by Paiva et al. [2] since it is the foundation of the models developed in this thesis regarding Multi-channel audio-based estimation of PEP. Data collection was provided by Centre for Informatics and Systems of the University of Coimbra (CISUC). The main methodological steps of Paiva et al. [2] model are summarized in Figure 8 and will be described in the following subsections.

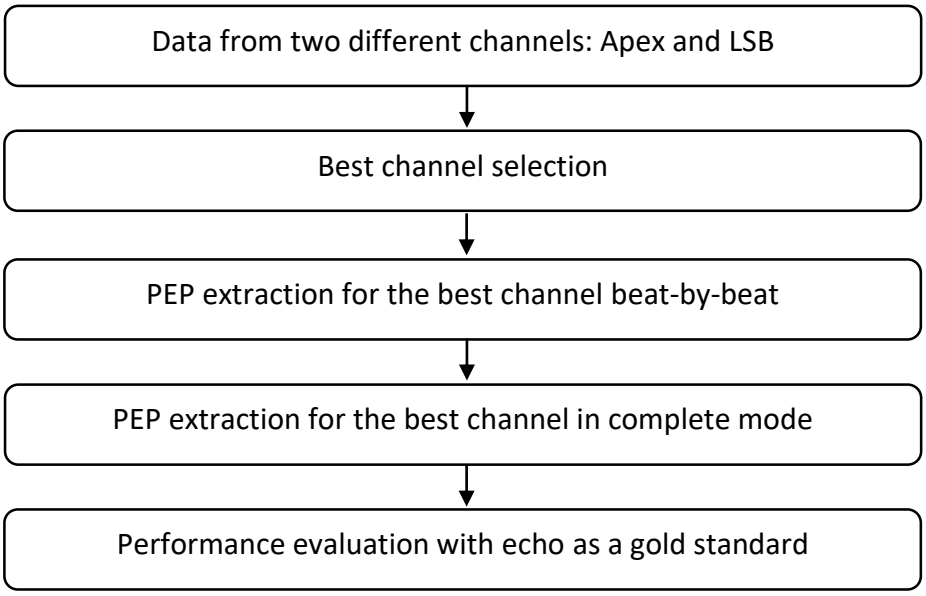


Figure 8 – Overview of Paiva et al. [2] model for a Multi-Channel Audio-Based Estimation of the PEP.

Apex and LSB represent two different body regions from where the heart sound was extracted. The existing method extracts information from both channels, choses the best and then extracts PEP for the best channel using only the parameters from that channel. The first goal of this thesis is to not discard the information extracted from the channel that had the worst performance, and to use it instead to get a better estimation accuracy of PEP for the best channel with a complete mode approach.

### 3.1.2 Experimental setup and data collection

Data acquisition was performed in the HeartSafe project from University of Coimbra [2]. Data collection involved 8 healthy male volunteers, and was carried out at “Centro Hospitalar de Coimbra”, where heart sounds (two channels) and echocardiographies (echo) were acquired simultaneously. It was also acquired a synchronous ECG with the mentioned signals, serving as a reference signal for co-registration. The average age from the population was 30.4 ± 9.8 years, the body mass index 25.9 ± 4.7 Kg/m$^2$ and the average heart rate was around 66.0 ± 14.9 bpm. All the measurements were conducted by an authorized medical specialist.

Patients were positioned in supine position, turned left (approximately 45º). The echo was configured for Doppler mode and the stethoscopes were positioned in the LSB and apex regions. Heart sound, echocardiogram and ECG were acquired with runs between 80 and 100 seconds. To acquire ECG and echocardiography they used a Vivid system from General Electric. To acquire heart sound and ECG they used two Meditron stethoscopes and an ADInstruments Bio Amp ECG recorder connected to an ADInstruments Powerlab. Heart sound and ECG were recorded at sampling frequency of 2 kHz.

Echo served as a gold standard to evaluate the accuracy of the algorithm extracting PEP, so after data acquisition, annotations of the opening instants of aortic valve were performed, with the associated PEP values. This procedure was made under the supervision of an experienced clinical expert in echocardiography.

### 3.1.3 Sound channel selection

As it was mentioned previously, sound was collected from two sites: the apex and left sternum border (LSB). The first step is to identify which channel has a better performance between those two.

The algorithm that performs the channel selection was developed by Paiva et al. [2] from University of Coimbra, so all credits for the following algorithm are given to him.

Paiva et al. [2] identified that one way to select the best channel was to determine the one with the highest signal-to-noise (SNR) ratio. To this end, he proposes a signal contrast feature, adapted from the spectral contrast feature proposed in [44].

This method is described in the following paragraphs and is performed for each heartbeat.

**Step 1.** Select the *audio segment* corresponding to the current heartbeat.

PEP is formally defined as the time interval between the Q-peak of the ECG to the opening of the aortic valve. Hence, an algorithm for detection of Q-peaks [45] is applied. The relevant audio segment starts at Q-peak time and as [1] suggests, has a duration of 210 ms.

**Step 2.** Compute the *amplitude contour* of the audio segment corresponding to the current heartbeat, for each sound channel.

The audio segment is full wave rectified and smoothed with a 100 msec half-Hanning window, described in (1):

$$c[n] = |s[n]| * W\left[n - \frac{W}{2}\right], n = 1,2, \dots, N \quad (1)$$

$$w[n] = 0.5 - 0.5\cos\left(\frac{2\pi(n-1)}{W-1}\right), n = 1,2, \dots, \frac{w}{2}$$

- $c[n]$ represents the amplitude contour of a given audio segment $s[n]$ with $N$ samples.
- $w[n]$ stands for the half- Hanning window.
- $W$ denotes the number of samples (corresponding to 100 msec at the employed 2kHz sampling frequency). Zero output delay is guaranteed by shifting the window.

**Step 3.** Determine the *signal contrast* of the amplitude contour segment corresponding to the current heartbeat, for each sound channel.

The amplitude contour $c[n]$ is returned as a vector. This vector is sorted into descending order of magnitude, forming a new vector $\{c1, c2, \dots, cN\}$ where $c1 \geq c2 \geq \dots \geq cN$. Equations (2) and (3) describe how the signal peak and valley are estimated, respectively.

$$peak = \frac{1}{\alpha N}\sum_{i=1}^{\alpha N} c_i \quad (2)$$

$$valley = \frac{1}{\alpha N}\sum_{i=1}^{\alpha N} c_{N-i+1} \quad (3)$$

$\alpha$ represents a neighborhood factor set to 0.2. Signal peak is calculated the average of 20% highest samples in the amplitude contour while signal valley corresponds to the 20% lowest.

Signal contrast (SC) corresponds to the difference between the computed signal peak, and valley, as described in equation (4).

$$SC = peak - valley \tag{4}$$

**Step 4.** Select the *best channel*.

The best channel is selected beat-to-beat, where a different channel might be selected each heartbeat. After beat-to-beat selection is performed, a complete mode is applied, where the channel that was selected the best channel in a higher number of beats, is considered as the best channel for every beat. Complete mode allows channel switching when the wrong channel is selected.

### 3.1.4 PEP estimation

For PEP estimation, a Bayesian approach is followed, resorting to the instantaneous amplitude (IA) of the HS waveform as the main feature. The algorithm was proposed by Paiva et al. [1], and its adapted in this thesis in every approach made to estimate PEP. This algorithm is the basis of this thesis, so it will be described in the following paragraphs. Any extra information about the algorithm can be find in [1].

The motivation for this approach comes up from the fact that the closure of AV valves is usually correlated with strong amplitude values in the first HS. According to [23], PEP is estimated based on the delay between AV closure and aortic valve opening. To constrain the range of possibilities, the previous heartbeat PEP interval in included in the model since abrupt variations should not occur while patients are at rest during data acquisition.

The model follows a two-pass approach. During the first iteration, it assumes initial probability distributions for the variables used, based on average population values reported in the literature. In the second pass, the probability distributions are updated based on the results obtained during the first pass. Therefore, the model is patient-dependent and applies a data-driven approach.

As described in **step 1** of the previous section, the same algorithm is used to detect Q-peaks.

Figure 9 summarizes the procedures carried out for PEP estimation. In the next paragraphs, each of the stages will be described.

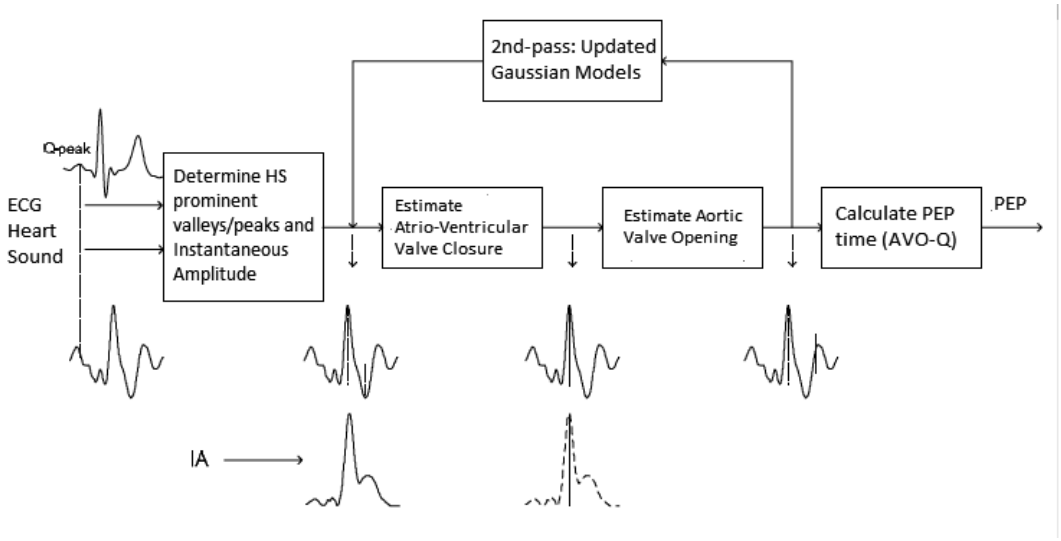


Figure 9 - Overview of the model proposed for PEP estimation by Paiva et al. [1].

**Step 1**. *First pass.* Given a HS signal, *s*(*t*), the algorithm for PEP estimation starts by determining the signal's IA, *a*(*t*), via the analytic signal as in (5). There, HT ( ⋅ ) denotes the Hilbert transform:

$$a(t) = |s(t) + jHT(s(t))| \tag{5}$$

**Step 2**. *AV valve closure estimation.* Next, for each heartbeat, *k*, the AV closure time interval, $AV_k$, is estimated. The corresponding Q-peak (previously determined) is employed as reference. To this end, a Bayesian model is applied according to (6), using the prominences ($prom_k$) of the HS near the Q-peak, the IA curve and the previous AV interval ($AV_{k-1}$).

$$p(AV_k|prom_k, IA_k, AV_{k-1}) \approx p(AV_k|prom_k).\, p(AV_k|IA_k).\, p(AV_k|AV_{k-1}) \tag{6}$$

A time interval was established for the AV time estimation, obtained experimentally and proved reliable. This time interval is represented by $D_{AV}$ = [Q-peak time, Q-peak time + 110 ms] and $AV_k$, $IA_k$, $AV_{k-1} \in D_{AV}$.

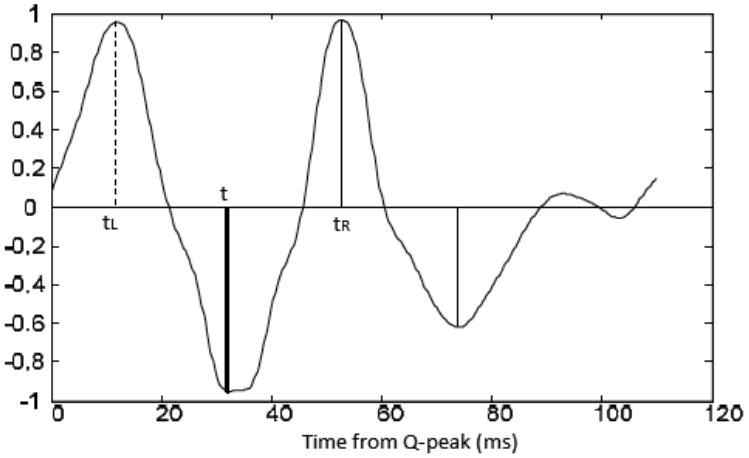


Figure 10 - Detection of prominences in the HS (vertical scale is arbitrary). [1]

The closing moment of the AV valves is strongly correlated with valleys and peaks of the HS, so in order to model *p* ($AV_k \mid prom_k$) from (6), the first step is to determine those events. To this end, an algorithm reported in [46] was applied according to (7). There, tL and tR represent the peaks from the left and from the right of the valley t.

$$prom_k(t) = \begin{cases} min(|s(t) - s(t_L)|, |s(t) - s(t_R)|) & t\ is\ peak/valley \\ 0 & otherwise \end{cases}, \qquad p(AV_k|prom_k) = \frac{prom_k}{\int_{t \in D_{AV}} prom_k dt}. \tag{7}$$

In (6), the conditional probability distribution of the AV closure time interval given the IA, $p(AV_k|IA_k)$, is defined as the normalized IA in beat *k*, according to (8).

$$p(AV_k|IA_k) = \frac{IA_k}{\int_{t \in D_{AV}} IA_k(t)} \tag{8}$$

The last probability distribution needed for (4), $p(AV_k|AV_{k-1})$, is modeled as in (9), a Gaussian distribution centered in the previous AV interval, $AV_{k-1}$, and with a standard deviation $\sigma_{AV}$ = 30 ms, motivated by results found in literature [47].

$$p(AV_k|AV_{k-1}) = G(AV_{k-1}, \sigma_{AV}) \quad (9)$$

Here, $G(\mu,\sigma)$ denotes a Gaussian function with mean value $\mu$ and standard deviation $\sigma$. However, in the first heartbeat there is no AV interval reference so a uniform distribution is employed. Finally, the AV interval is estimated as the time instant that maximizes (6).

**Step 3.** *PEP estimation.* After AV closure interval estimation, PEP duration, $PEP_k$, is inferred. Again, a Bayesian strategy is followed, employing the estimated AV interval in beat *k*, $AV_k$, and the previous PEP interval in beat *k* − 1, $PEP_{k-1}$, as in (10):

$$p(PEP_k|AV_k, PEP_{k-1}) \approx p(PEP_k|AV_k).p(PEP_k|PEP_{k-1}) \quad (10)$$

$$where\ AV_{k-1} \in D_{AV}\ and\ PEP_k, PEP_{k-1} \in\ D_{PEP}$$

$D_{PEP}$ denotes the time range PEP time estimation, corresponding to the time interval $D_{PEP}$ = [Q-peak time, Q-peak time + 210 ms]. As before, this interval was obtained experimentally and proved reliable.

The conditional probability distribution of PEP duration given the AV time interval, $p(PEP_k|AV_k)$, is modeled as a Gaussian centered in $AV_k + \mu_{PEP-AV}$ ($\mu_{PEP-AV}$ = 30 ms), with a standard deviation $\sigma_{PEP-AV}$= 30 ms motivated by result found in literature [23], suggesting that AV opening occurs typically 30 ms after AV closure.

$$p(PEP_k|AV_k) = G(AV_k + \mu_{PEP-AV}, \sigma_{PEP-AV}) \quad (11)$$

The PEP interval in beat *k*, $PEP_k$, knowing PEP from the previous beat, $PEP_{k-1}$, is modeled as a Gaussian centered in $PEP_{k-1}$, with a standard deviation $\sigma_{PEP}$ = 30 ms as in (12). Again, there is no PEP interval reference for the first heartbeat, so a uniform distribution is initially taken.

$$p(PEP_k|PEP_{k-1}) = G(PEP_{k-1}, \sigma_{PEP}) \quad (12)$$

Finally, the PEP interval is estimated as the time instant that maximizes (10).

$$PEP = \max\big(p(PEP_k|AV_k, PEP_{k-1})\big) \quad (13)$$

Gaussian models only serve for bootstrapping the identification processes, so a second pass is applied using a data-driven approach.

**Step 4.** *Second pass.* In the second pass the algorithm is run again with updated models. Mean and standard deviation values of *p* $(AV_k|AV_{k-1})$, $p(PEP_k|PEP_{k-1})$ and $p(PEP_k|AV_k)$, are updated using the obtained results. Also, the estimated AV and PEP distributions, $p(AV_k|prom_k, IA_k, AV_{k-1})$ and $p(PEP_k|AV_k, PEP_{k-1})$ are added to the model, resulting in equations (14) and (15). There, $p_{fp}$ stands for the distributions obtained with the first iteration of the algorithm.

$$p(AV_k|prom_k, IA_k, AV_{k-1}) \approx p(AV_k|prom_k).p(AV_k|IA_k).p_{fp}(AV_k|AV_{k-1}).p_{fp}(AV_k|prom_k, IA_k, AV_{k-1}) \quad (14)$$

$$p(PEP_k|AV_k, PEP_{k-1}) \approx p_{fp}(PEP_k|AV_k).\, p_{fp}(PEP_k|PEP_{k-1}).\, p_{fp}(PEP_k|AV_k, IA_k, PEP_{k-1}) \quad (15)$$

Finally, PEP is extracted as the time instant that maximizes (15), as described in (13).

Like it was mentioned previously, this model discards the information acquired from the worst channel, and the goal of the first step of this thesis was to use the discarded information to improve PEP estimation for the best channel. To this end, two approaches were performed and will be described in the following paragraphs.

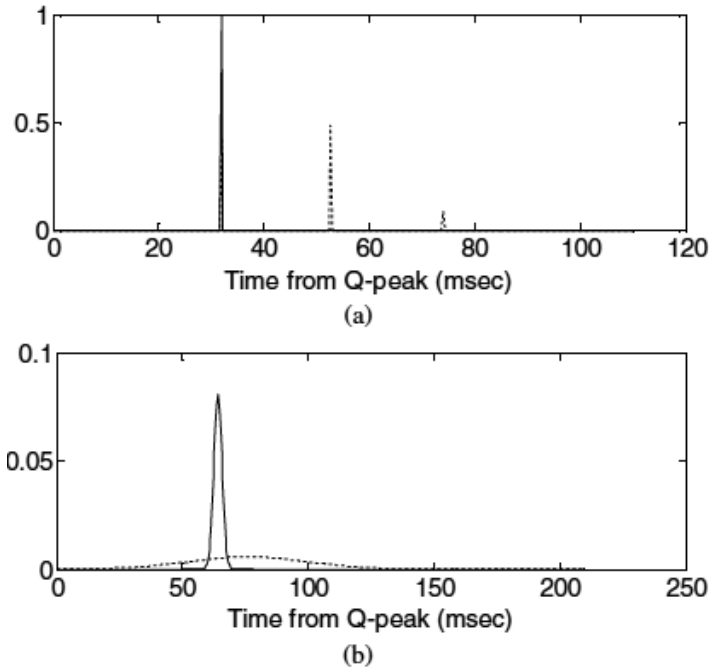


Figure 11 - (a) AV closure probability distribution; (b) PEP probability distribution. The dashed lines represent the probability distributions after the first pass of the algorithm. The solid lines denote the final distributions. [1]

## 3.2 Multi-channel Audio-based Estimation of PEP from the best channel using probability distributions from the worst channel

As mentioned previously, the main objective of the first stage of this thesis is to use the information extracted from the worst channel to improve the accuracy of PEP estimation for best channel. To this end, a Bayesian approach is performed based in the model described in section 3.1. To the existing model, three probability distributions with information of the worst channel were added, resulting in a model that takes in consideration the information from both channels in order to extract PEP from the best channel. Summarizing this model, it is possible to say that the algorithm described in section 3.1.4 is applied twice each beat.

Figure 12 shows an overview of the steps of the proposed model, that will be described in this section.

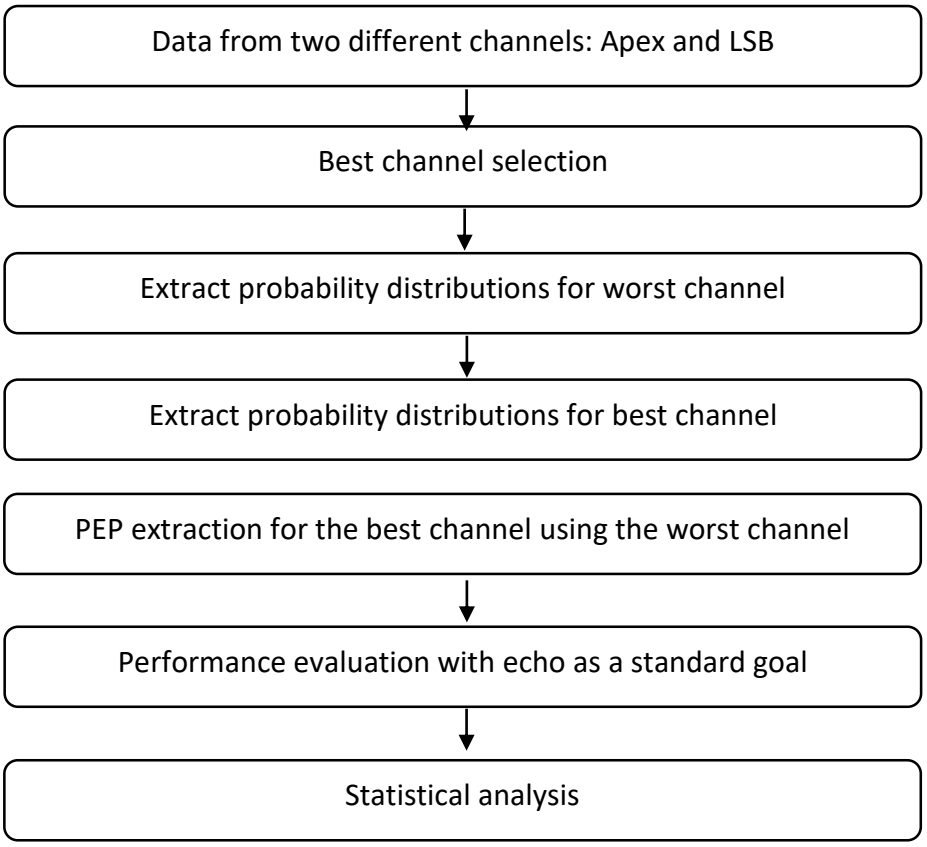


Figure 12 – Overview of the proposed model to extract PEP from best channel, using information from the worst channel in the form of probability distributions.

**Step 1** - Perform *Channel selection.*

Channel selection is performed using the algorithm described by equations (1), (2), (3) and (4) in section 3.1.3. The channel selection was made beat-by-beat, and after the channel that was selected the higher number of times was labeled the best, and the other worst. Knowing the best and the worst channel, the necessary probability distributions from the worst channel were extracted.

**Step 2** – Extraction of *probability distributions* for worst channel.

According to the model described in 3.1.4, PEP is extracted as in (15):

$$p(PEP_k|AV_k, PEP_{k-1}) \approx p_{fp}(PEP_k|AV_k).\, p_{fp}(PEP_k|PEP_{k-1}).\, p_{fp}(PEP_k|AV_k, IA_k, PEP_{k-1}) \quad (15)$$

As so, all the necessary probability distributions for PEP extraction regarding the worst channel are estimated using the algorithm described in 3.1.4:

- Probability distribution of PEP given AV time interval of the worst channel ($p_{worstchannel}(PEP_k|AV_k)$);
- Probability distribution of PEP given PEP from last heartbeat of the worst channel ($p_{worstchannel}(PEP_k|PEP_{k-1})$);
- Probability distribution of PEP given AV time interval, instantaneous amplitude and PEP from last heartbeat of the worst channel ($p_{worstchannel}(PEP_k|AV_k, IA_k, PEP_{k-1})$).

**Step 3**- Extraction of *probability distributions* for best channel.

This step is very similar to step 2, where the algorithm described in 3.1.4 is applied to extract the following probability distributions regarding the best channel:

- Probability distribution of PEP given AV time interval of the best channel ($p_{bestchannel}(PEP_k|AV_k)$);
- Probability distribution of PEP given PEP from last heartbeat of the best channel ($p_{bestchannel}(PEP_k|PEP_{k-1})$);
- Probability distribution of PEP given AV time interval, instantaneous amplitude and PEP from last heartbeat of the best channel ($p_{bestchannel}(PEP_k|AV_k, IA_k, PEP_{k-1})$).

**Step 4**- Extract *PEP* for best channel.

With the required probability distributions extracted, at this point is possible to start PEP extraction for the best channel.

To use information from the worst channel to extract PEP from the best channel, we assumed independence between the channels, such as:

$$p(A \cap B) = p(A).p(B) \tag{16}$$

As so, PEP from the best channel is estimated as the multiplication of the probability distributions from the best channel and the probability distributions from the worst channel, resulting in equation (17):

$$p\left(PEP_{k_{bestchannel}}|AV_{k_{bestchannel}}, PEP_{k-1_{bestchannel}}, AV_{k_{worstchannel}}, PEP_{k-1_{worstchannel}}\right) \tag{17}$$
$$\approx p_{fp_{bestchannel}}(PEP_k|AV_k).p_{fp_{bestchannel}}(PEP_k|PEP_{k-1}).p_{fp_{bestchannel}}(PEP_k|AV_k, IA_k, PEP_{k-1})$$
$$.p_{fp_{worstchannel}}(PEP_k|AV_k).p_{fp_{worstchannel}}(PEP_k|PEP_{k-1}).p_{fp_{worstchannel}}(PEP_k|AV_k, IA_k, PEP_{k-1})$$

PEP is then obtained as time instant that maximizes (17):

$$PEP_{bestchannel} = \max\left(p\left(PEP_{k_{bestchannel}} \middle| AV_{k_{bestchannel}}, PEP_{k-1_{bestchannel}}, AV_{k_{worstchannel}}, PEP_{k-1_{worstchannel}}\right)\right) \quad (18)$$

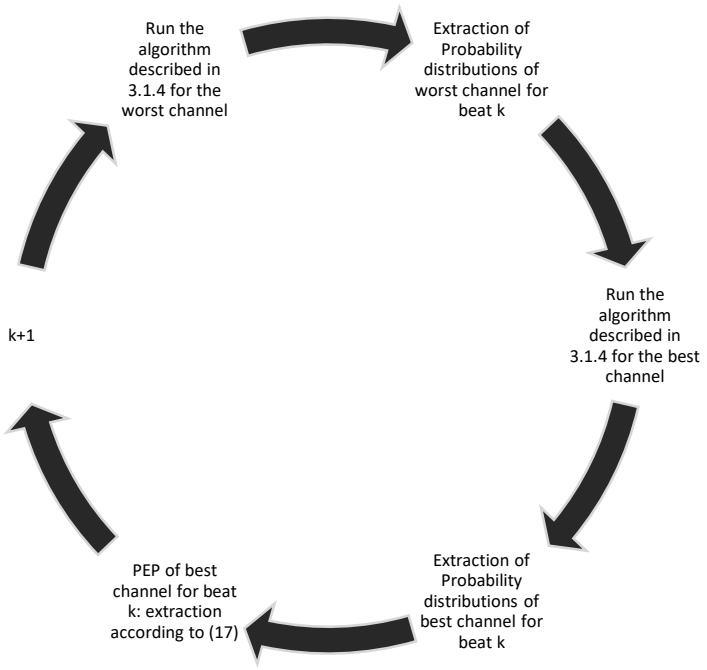


Figure 13- Summary of the model proposed for PEP extraction using probability distributions from the worst channel.

Figure 13 describes the proposed model, and how it applies the algorithm from section 3.1.4 to extract PEP for the best channel.

## 3.3 Multi-channel Audio-based Estimation of PEP from the best channel using PEP from the worst channel

The independence between both channels is a strong affirmation, and might be unreliable, so in this approach we consider that the two channels are dependent between each other. As this model still follows a Bayesian approach based in the model described in section 3.1, in this approach we used PEP directly from the worst channel. To summarize it, a new parameter was added to the existing model described in 3.1, in the form of a Gaussian centered in the PEP value of the worst channel. Like the last approach, it is possible to say that the algorithm described in 3.1.4 is applied twice each beat, once for each channel.

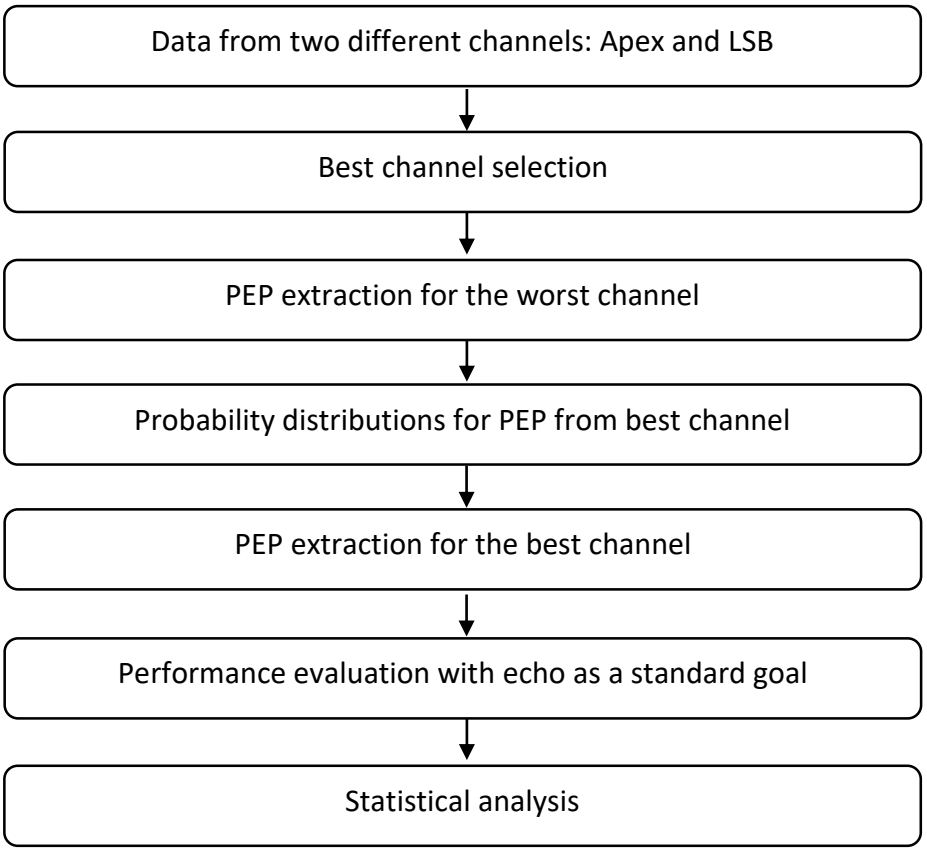


Figure 14 – Overview of the proposed model to extract PEP from best channel, using information from the worst channel in the form of a Gaussian centered in PEP from the worst channel.

**Step 1** - Perform *Channel selection*.

Channel selection is performed using the algorithm described in chapter 3.1.3. The channel selection was made beat-by-beat, and after the channel that was selected the higher number of times was labeled the best, and the other worst.

**Step 2** – *PEP extraction* for worst channel.

According to the algorithm described in 3.1.4, PEP is extracted and the time that maximizes equation (15):

$$p(PEP_k|AV_k, PEP_{k-1}) \approx p_{fp}(PEP_k|AV_k).\, p_{fp}(PEP_k|PEP_{k-1}).\, p_{fp}(PEP_k|AV_k, IA_k, PEP_{k-1}) \quad (15)$$

This model is applied to data from the worst channel, with the final result being a PEP value for each beat:

$$PEP_{worstchannel} = \max\big(p(PEP_k|AV_k, PEP_{k-1})\big) \quad (19)$$

**Step 3** – Initialization of the *Gaussian*.

In this step, a new probability distribution is created, defined as a Gaussian centered in $PEP_{worstchannel}$:

$$p(PEP_{worstchannel}) = G(PEP_{worstchannel}, \delta), where\ \delta = 30\ ms \quad (20)$$

***Step 4***- Extraction of *probability distributions* for best channel.

The algorithm described in 3.1.4 is applied to extract the following probability distributions regarding the best channel:

- Probability distribution of PEP given AV time interval of the worst channel ($p_{bestchannel}(PEP_k|AV_k)$);
- Probability distribution of PEP given PEP from last heartbeat of the worst channel ($p_{bestchannel}(PEP_k|PEP_{k-1})$);
- Probability distribution of PEP given AV time interval, instantaneous amplitude and PEP from last heartbeat of the worst channel ($p_{bestchannel}(PEP_k|AV_k, IA_k, PEP_{k-1})$).

**Step 5**– *PEP extraction* for the best channel.

The new parameter in the form of a Gaussian centered in PEP from the worst channel, is added to the model described in (15). As so, the new model using information from the worst channel to extract PEP of the best channel is described in (21):

$$p\left(PEP_{k_{bestchannel}}|AV_{k_{bestchannel}}, PEP_{k-1_{bestchannel}}, PEP_{k_{worstchannel}}\right) \approx p_{fp_{bestchannel}}(PEP_k|AV_k).p_{fp_{bestchannel}}(PEP_k|PEP_{k-1}).p_{fp_{bestchannel}}(PEP_k|AV_k, IA_k, PEP_{k-1}) .p\left(PEP_{k_{worstchannel}}\right) \quad (21)$$

PEP is then obtained as time instant that maximizes (21) according to (22):

$$PEP_{bestchannel} = \max\left(p\left(PEP_{k_{bestchannel}}|AV_{k_{bestchannel}}, PEP_{k-1_{bestchannel}}, PEP_{k_{worstchannel}}\right)\right) \quad (22)$$

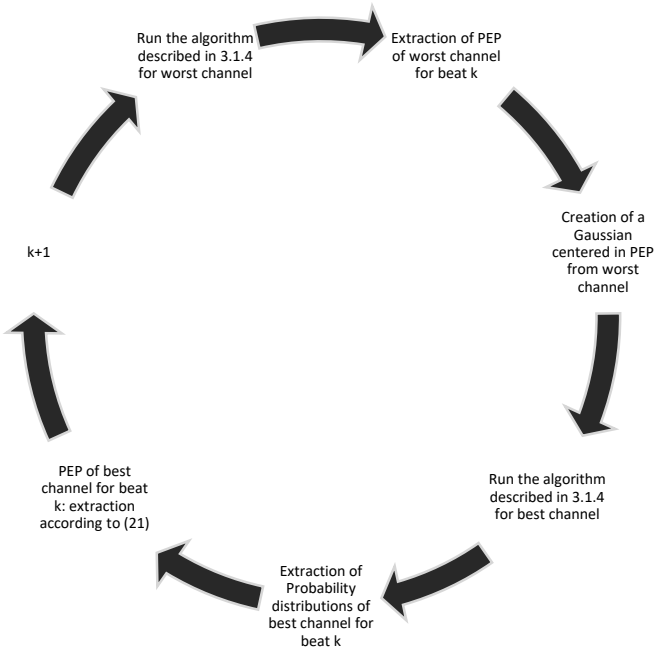


Figure 15 - Summary of the model proposed for PEP extraction using a Gaussian centered in PEP from the worst channel.

Figure 15 represents que model applied in this section, and summarizes how the Bayesian model described in 3.1.4 is applied to extract PEP from the best channel, using information from the worst channel.

## 3.4 Single-channel Audio-based Estimation of PEP using PPG

### 3.4.1 Overview

In this model, we introduce a new data collection, containing only information about one channel. In the other hand, the new data collection has PPG information, which allow us to use this signal to improve PEP extraction. The idea behind this model is to extract PEP from PPG, and use it as a parameter to influence the PEP calculation based in heart sound. To this end, the algorithm described in 3.1.4 is adapted, with the addition of a new probability distribution of PEP, extracted from PPG. To this end, an algorithm reported by Couceiro et al. [48] is used in order to extract LVET from PPG, that is after used to assess a value of PEP. The procedure of extraction of PEP from PPG will be described in this section sections, alongside each step of this model. In order to evaluate the results obtained,

the algorithm described 3.1.4 is applied to the new data collection. As the data collection only contains information about one channel, there is no need to perform a channel selection.

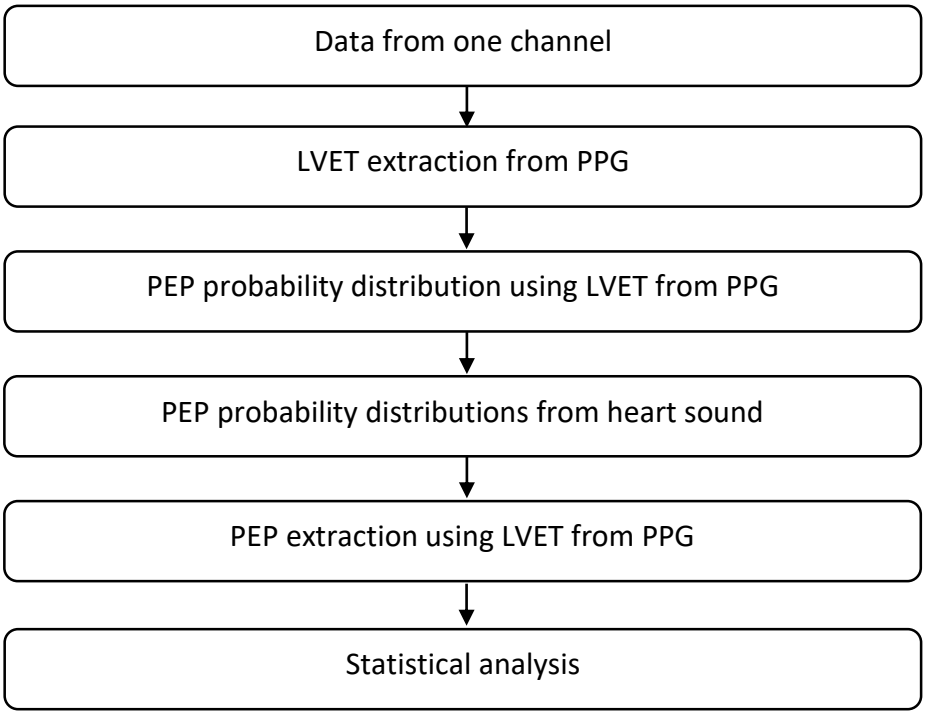


Figure 16- Overview of the proposed model for Single-channel audio-based PEP extraction using PPG.

### 3.4.2 Experimental setup and data collection

As the new data collection only contains information for one channel, it is not necessary to perform best channel selection. Therefore, PEP estimation is applied as soon as the data collection is available. The model will be described in the next paragraphs.

As the last data collection, described in 3.1, this data acquisition was conducted at “Centro Hospitalar de Coimbra”. PPG and echocardiography were acquired simultaneously, with an ECG acquisition serving as a reference of the co-registration procedure [49]. The data collected involved 68 subjects including healthy individuals and people suffering from CVD [49]. For this thesis, we used a smaller data collection, using a set of 16 acquisitions from four healthy people, all males. Thus, there was four different acquisitions for each patient. The individuals studied were randomly selected.

As in the previous data collection, the measurement protocol was conducted by an authorized specialist [49]. Echocardiography was acquired in Doppler mode and the annotation of aortic opening and closure times in echo was performed by an experienced clinical expert. PPG was collected at the right hand index finger [49].

### 3.4.3 PEP estimation

The main goal of this model is to use features extracted from PPG to help in the audio-based PEP extraction. To this end, we used LVET extracted from PPG to create a probability distribution of PEP. Two approaches were made in this scenario, which will be explained in the following sub-chapters.

The first model created is an adaptation of the model from [1] described in section 3.1.4, adding a new probability distribution to the final equation (15) of PEP estimation. This model is described in this section.

As in the multi-channel approaches described previously, the algorithm reported in [45] was applied for the detection of Q-peaks.

**Step 1** – *LVET extraction* from PPG.

LVET measure was performed using a model proposed by Couceiro et al. [48]. This method outputs some important variables, between which we highlight LVET and PPG peaks time, which were the ones we used for this model.

This model is composed by four steps, described in Figure 17.

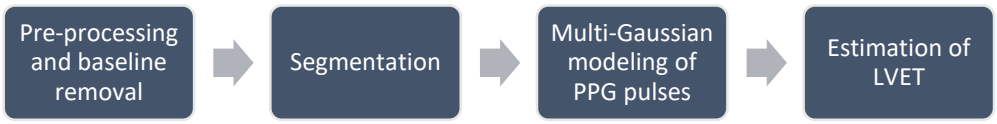


Figure 17- Overview of the proposed model for LVET extraction by Couceiro et al. [48] .

Since PPG can be susceptible to many factors, a pre-processing is applied in order to minimize their possible effect in the next phases. Then, a segmentation of PPG is performed in order to match each PPG peak to a single heartbeat. The third step uses a model composed by five Gaussian functions, where an additional pre-processing is performed and PPG is decomposed into its main physiological components. LVET is then estimated from the analysis of this components. Any extra information about the model can be found in [48].

**Step 2**- Extraction of *S2 start* times.

S2 start times were extracted using a model proposed by Paiva et al. [1]. The goal of this model is to segment the HS waveform into a number of candidates for S2 sound segments. To this end, the algorithm resorts to the application of Shannon energy operator to detail coefficients of the fast wavelet transform(FWT).

**Step 3**- *Synchronization* of LVET values with corresponding S2 starts.

The number of LVET values, S2 starts and heart beats detected differed between themselves, suggesting a need of synchronization. In order to guarantee that the LVET values we were using corresponded to the correct S2 start and beat from HS, we established some constraints:

$$R_{ECG}^{k} \leq Peak_{PPG} \leq R_{ECG}^{k+1} \quad (23)$$

$$R_{ECG}^{k} \leq S2start_{HS} \leq R_{ECG}^{k+1} \quad (24)$$

$$Peak_{PPG} \leq S2start_{HS} \quad (25)$$

As it is possible to see in Figure 5 usually the PPG peak corresponding to beat k comes after the corresponding R-peak from ECG and before the R-peak of the next beat, resulting in equation (23).

As Figure 3 demonstrates, S2 start is represented by the t-wave of an ECG, therefore it happens after R-peak of the corresponding beat (24). At the same time, to guarantee that S2 start value and PPG peak correspond to the same beat, they must meet these conditions for the same beat. Looking at Figure 5 its notable that PPG peak usually occurs at the same time as T wave begins, and using information from Figure 3 we can see that S2 starts occurs in the decreasing stage of T wave, so usually PPG peak occurs slightly before S2 start. To prevent situations where multiple PPG peaks meet the required conditions for each S2 start, equation (25) is applied as a constraint.

**Step 4**- *PEP probability distribution.*

Each heart beat is now corresponded with a LVET value, a S2 start and a Q-peak time. As it was mentioned, PEP is the interval between the start of ventricular depolarization (Q-peak) and aortic valve opening, and LVET is the interval between aortic valve opening and its closure. Based on that, PEP and LVET can be seen in Figure 3.

As so, PEP can be calculated as described in equation (26).

$$PEP_{value}(k) = S2_{start}(k) - LVET_{value}(k) - Q_{peak}(k) \quad (26)$$

From the estimated PEP value for each peak, we created a new probability distribution in the form of a Gaussian described in (27):

$$p(PEP_{PPG}) = G(PEP_{value}, \delta) \quad (27)$$

$PEP_{value}$ represents the center of the Gaussian according to calculations performed in (26), and δ its standard deviation settle to δ=30 ms according to the literature as it was mentioned previously.

**Step 5**- Extraction of probability distributions from heart sound.

The algorithm described in 3.1.4 is applied to extract the following probability distributions of PEP:

- Probability distribution of PEP given AV time interval (p($PEP_k|AV_k$));
- Probability distribution of PEP given PEP from last heartbeat ($p(PEP_k|PEP_{k-1})$);
- Probability distribution of PEP given AV time interval, instantaneous amplitude and PEP from last heartbeat ($p(PEP_k|AV_k, IA_k, PEP_{k-1})$).

**Step 6** – *PEP extraction.*

Adapting the model described in 3.1.4, the probability distribution of PEP extracted from PPG is added, resulting in equation (28):

$$(PEP_k|AV_k, PEP_{k-1}, PEP_{PPG}) \approx p_{fp}(PEP_k|AV_k).p_{fp}(PEP_k|PEP_{k-1}).p_{fp}(PEP_k|AV_k, IA_k, PEP_{k-1}).p(PEP_{PPG}) \quad (28)$$

The final value of PEP is then calculated as the time that maximizes (27):

$$PEP = \max(p(PEP_k|AV_k, PEP_{k-1}, PEP_{PPG})) \quad (29)$$

In order to see if the new probability distribution ($p(PEP_{PPG})$) was having a positive effect in PEP calculation, the influence of the parameter was increased by reducing the standard deviation of the Gaussian. As so, all the steps mentioned above were repeated δ=15ms. The lower the value of δ, the

more influence will the distribution have in the final extraction of PEP, but its value was fixed in δ=15ms since we are aware of the error propagation resulting from steps 1, 2 and 4. To better understand the proposed model, Figure 18 summarizes all the steps taken to extract PEP using PPG.

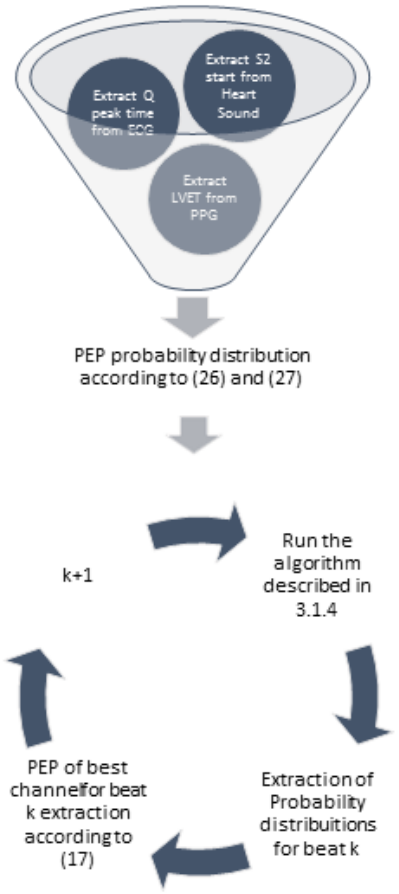


Figure 18- Summary of the proposed model for PEP extraction using PPG.

### 3.4.4 Single channel Audio-based Estimation of PEP using PPG: second approach

The second approach applied to extract PEP was very similar to the last one described in 3.4.3. The idea behind this model was to not limit PEP variations from beat to beat while still using PEP from PPG as a parameter to extract PEP. As so, the difference between this model and the last one, is that this model does not used the probability distribution of PEP knowing the PEP from the last beat ($p(PEP_k|PEP_{k-1})$). As so, step 1,2,3 and 4 of the last model were repeated and the following steps can be found below:

**Step 5**- Extraction of *probability distributions* from heart sound.

The algorithm described in 3.1.4 is applied to extract the following probability distributions of PEP:

- Probability distribution of PEP given AV time interval of worst channel ($p(PEP_k|AV_k)$*);*
- Probability distribution of PEP given AV time interval and instantaneous amplitude of worst channel ($p(PEP_k|AV_k, IA_k)$).

**Step 6** – *PEP extraction.*

Adapting the model described in 3.1.4, the probability distribution of PEP extracted from PPG is added, resulting in equation (30):

$$(PEP_k|AV_k, IA_k, PEP_{PPG}) \approx p_{fp}(PEP_k|AV_k).p_{fp}(PEP_k|AV_k, IA_k).p(PEP_{PPG}) \quad (30)$$

The final value of PEP is then calculated as the time that maximizes (30):

$$PEP = \max(p(PEP_k|AV_k, IA_k, PEP_{PPG})) \quad (31)$$

As in section 3.4.3, in order to evaluate how the new probability distribution was affecting PEP calculation, all the steps referred above were repeated a different standard deviation for $p(PEP_{PPG})$ (δ=15 ms).

# Chapter 4

# Results and Discussion

## 4.1 Multi channel Audio-Based Estimation of PEP

### 4.1.1 Existing model

As the main goal of this thesis was to improve the accuracy of an audio based extraction of PEP reported by Paiva et al. [2] it's important to evaluate its results first, in order to compare the results obtained using the new models with those already established. In this section, the results obtained in [2] for multi-channel audio-based estimation of PEP are detailed according to what was reported.

Table 8 - PEP median, mean and standard deviation results from Paiva et al. [2] in ms.

| **PEP estimation results (ms)** | |
|---|---|
| Median | 65.5 |
| Mean | 67.3792 |
| Standard Deviation | 6.2356 |

Table 9 - PEP error mean and standard deviation results from Paiva et al. [2], in ms.

| **Error estimation results (ms)** | |
|---|---|
| Mean | 9.2692 |
| Standard Deviation | 7.1457 |

The correlation value between PEP values extracted and PEP values from echo (golden standard) was 0.465.

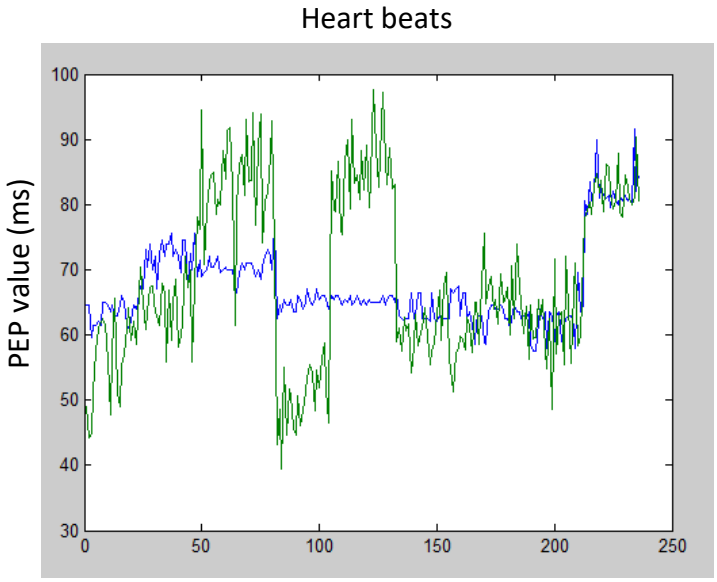


Figure 19- Results from PEP(blue) and echo(green) values from Paiva et al. [2].

In order to perform a statistical analysis regarding the results from the new models, it is necessary to know if the distribution of the error of the existing results is Gaussian. To this end, a Kolmogorov-Smirnov test was applied with a significance level of 5% as default, revealing that the error distribution is Gaussian.

### 4.1.2 Best results obtained with Multi-channel models

In this section the best results obtained with each model regarding a multi-channel approach are detailed.

#### 4.1.2.1 Multi-channel Audio-based Estimation of PEP from the best channel using probability distributions from the worst channel

This sub-section details the results obtained using the model described in 3.2. This model uses three probability distributions ($p_{worstchannel}(PEP_k|AV_k)$, $p_{worstchannel}(PEP_k|PEP_{k-1})$), $p_{worstchannel}(PEP_k|AV_k, IA_k, PEP_{k-1})$ to extract PEP. Table 10 summarizes the results obtained for the PEP value, while Table 11 is related with the error in the calculation of PEP.

Table 10 - PEP median, mean and standard deviation results from Multi-channel audio based PEP extraction from best channel using probability distributions from the worst channel, in ms.

| **PEP estimation results (ms)** | |
|---|---|
| Median | 68.5 |
| Mean | 68.5445 |
| Standard deviation | 6.5559 |

Table 11 - PEP error mean and standard deviation results from Multi-channel audio based PEP extraction from best channel using probability distributions from the worst channel, in ms.

| **Error estimation results (ms)** | |
|---|---|
| Mean | 9.4062 |
| Standard deviation | 7.4379 |

The correlation value between PEP values extracted and PEP values from echo (golden standard) was 0.420.

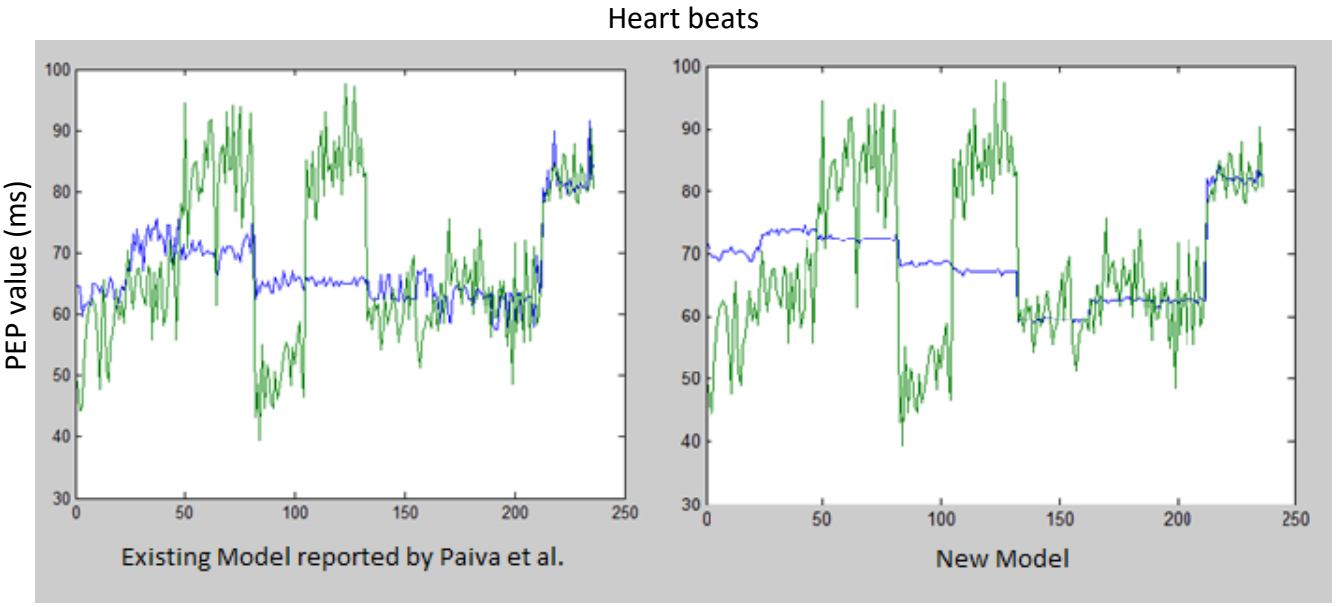


Figure 20 - Comparison of the results from the model detailed in 3.1.4 with the new model described in section 3.2. (PEP(blue) and echo(green)).

It is possible to see a slightly decrease in the algorithm accuracy, which is notable in Figure 20, where the extracted PEP by the new model does not follow PEP from echo with the same quality. Although the calculated PEP with the new model follows a very close pattern to the existing model, it is clear that PEP values between each beat are do not vary as much as its supposed, suggesting $PEP_{k-1}$ has a stronger influence in $PEP_k$ than previously. Also, the correlation value between PEP extracted and PEP from echo decreases, confirming the decrease in the accuracy of PEP extraction using the new model. Even then, a statistical analysis between the error of both models is performed to verify if the difference between the models is statistically significant. To this end, a Kolmogorov-Smirnov test was applied to the error distribution of the new model, that was found to be Gaussian. As so, a paired T-test was carried out and the results achieved with the new model proved to be statistical significant ($p - value = 3.2979 \times 10^{-7} < 0.01$). Considering the error increase from 9.27 ms to 9.41 ms (1.5%), we can conclude that this model does not need to be discarded, as it has room for improvement and has potential to improve the existing results.

### 4.1.2.2 Multi-channel Audio-based Estimation of PEP from the best channel using PEP from the worst channel

In this section, we can see the results obtained using a Gaussian centered in the PEP value from the worst channel, to extract PEP from the best channel. The Gaussian is updated every beat, using the PEP from beat k of the worst channel, to extract the PEP of beat k of the best channel. Standard deviation is settled as 30 ms in this section as that was the one that presented the best results for this model. Table 12 summarizes the results obtained for the PEP value, while Table 13 is related with the error in the calculation of PEP.

Table 12 - PEP median, mean and standard deviation results from Multi-channel audio based PEP extraction from best channel using PEP from the worst channel, in ms. δ=30.

| **PEP estimation results (ms)** | |
|---|---|
| Median | 68.5 |
| Mean | 68.4470 |
| Standard deviation | 6.4780 |

Table 13 - PEP error mean and standard deviation results Multi-channel audio based PEP extraction from best channel using PEP from the worst channel, in ms. δ=30.

| **Error estimation results (ms)** | |
|---|---|
| Mean | 9.5064 |
| Standard deviation | 7.3242 |

The correlation value between PEP values extracted and PEP values from echo (golden standard) was 0.418.

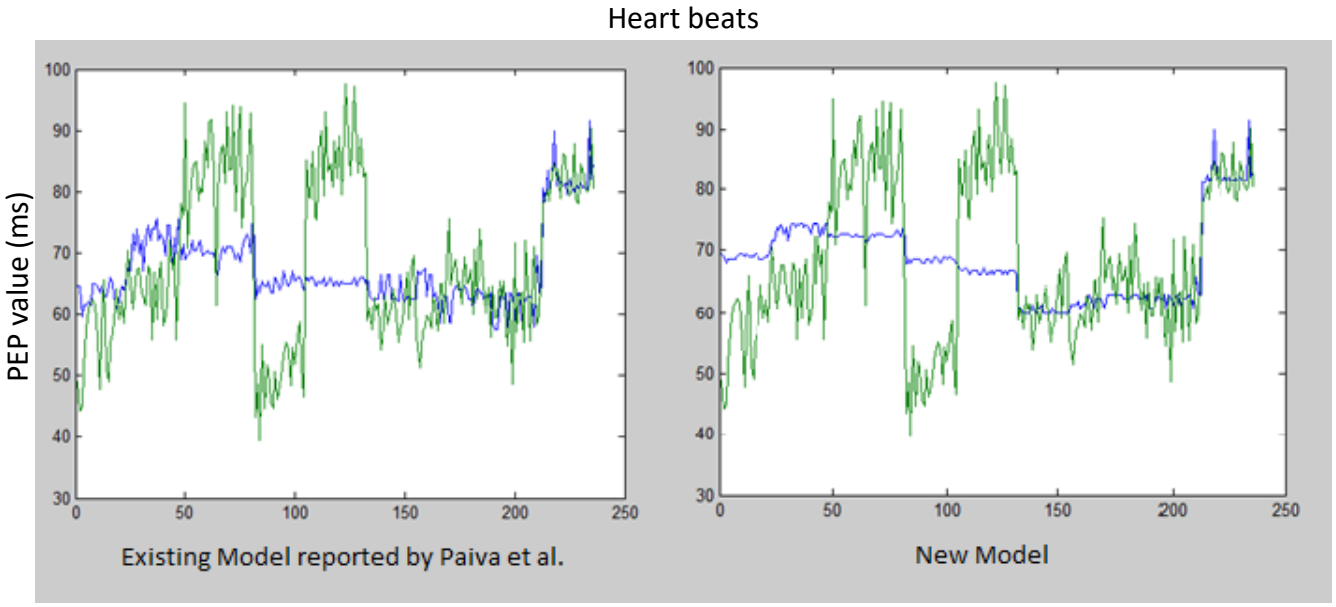


Figure 21 - Comparison of the results from the model detailed in 3.1.4 with the model described in 3.3 using δ= 30 ms (PEP(blue) and echo(green)).

This approach shows results very close to the ones in section 4.1.1, increasing the error of PEP extraction slightly. Across all beats, it is possible to see in Figure 21 that the new model follows a very similar pattern to the existing model. Once again, PEP seems to not vary very much in consecutive beats, excluding the biggest variations. This monotony suggests PEP from the last beat is having a bigger influence in PEP of the current beat, and seems to be limiting its variation. As the last model, this one also presents a decrease in the correlation value between PEP extracted and PEP from echo, which corroborates the decrease in accuracy of PEP extraction. The results from this model, are worse than the ones obtained with model described in section 3.2, suggesting that using PEP directly from worst channel to extract PEP from the best channel is not a good procedure. A statistical analysis was performed in order to evaluate the statistical significance of the difference between this model and the one reported by Paiva et al. [2]. Error distribution was found to be Gaussian. Therefore, a paired T-test was applied to compare the models and the results proved to be statistically significant, with a $p - value = 2.7690 \times 10^{-9} < 0.01$. The results suggest the model was not performing according to what is expected, and therefore the model was applied one more time with different parameters in order to evaluate where was the problem. The second application of the model will be described forward in this document.

## 4.2 Single-channel Audio-based Estimation of PEP using PPG

### 4.2.1 Existing model

As referred previously, the new models adapt the algorithm reported in [1] include PPG in the model. As so, this section describes the results obtained using the model from [1] without the inclusion of PPG, and served as a standard to evaluate the improvement of the new models.

Table 14 - PEP median, mean and standard deviation results from the existing algorithm [1], in ms.

| **PEP estimation results (ms)** | |
|---|---|
| Median | 73 |
| Mean | 73.3952 |
| Standard deviation | 3.0868 |

Table 15 - PEP error mean and standard deviation results from existing algorithm [1], in ms.

| **Error estimation results (ms)** | |
|---|---|
| Mean | 6.1695 |
| Standard deviation | 4.3691 |

The correlation value between PEP values extracted and PEP values from echo (golden standard) was 0.553.

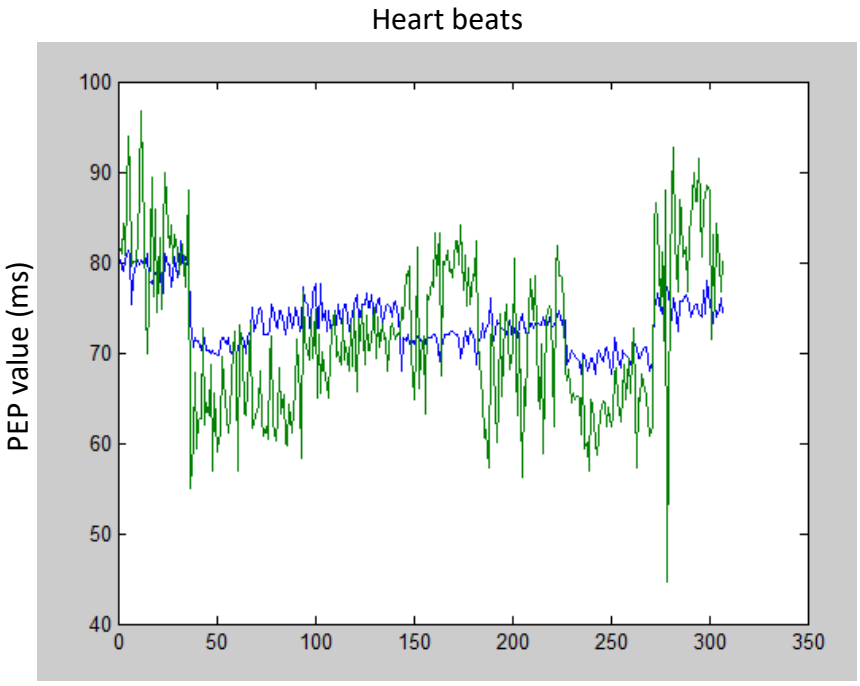


Figure 22 - Results from PEP(blue) and echo(green) values from the single-channel audio-based PEP extraction using the Paiva et al. [1] algorithm.

### 4.2.2 Best results obtained with Single-channel models

In this section the best results obtained for each model created for a single-channel approach are detailed.

#### 4.2.2.1 Single-channel Audio-based Estimation of PEP using PPG

This section is dedicated to evaluate the results obtained with the model described in 3.4.3 with the standard deviation for the Gaussian used settled in 15 ms. This procedure was the one that delivered the best results amongst all the different approaches for the single-channel audio-based PEP estimation using PPG. The main goal of the analysis of this results to evaluate if using PPG to extract PEP is a good procedure. Result regarding the values of PEP extracted can be seen in Table 16 and the corresponding error in Table 17.

Table 16 - PEP median, mean and standard deviation results from Single channel audio-based PEP estimation using PPG, in ms: model from 3.4.3, δ=15.

| **PEP estimation results (ms)** | |
|---|---|
| Median | 73.33 |
| Mean | 71.5483 |
| Standard deviation | 4.5717 |

Table 17 - PEP error mean and standard deviation results Single channel audio-based PEP estimation using PPG, in ms: model from 3.4.3, δ=15.

| **Error estimation results (ms)** | |
|---|---|
| Mean | 5.4110 |
| Standard deviation | 4.1260 |

The correlation value between PEP values extracted and PEP values from echo (golden standard) was 0.630.

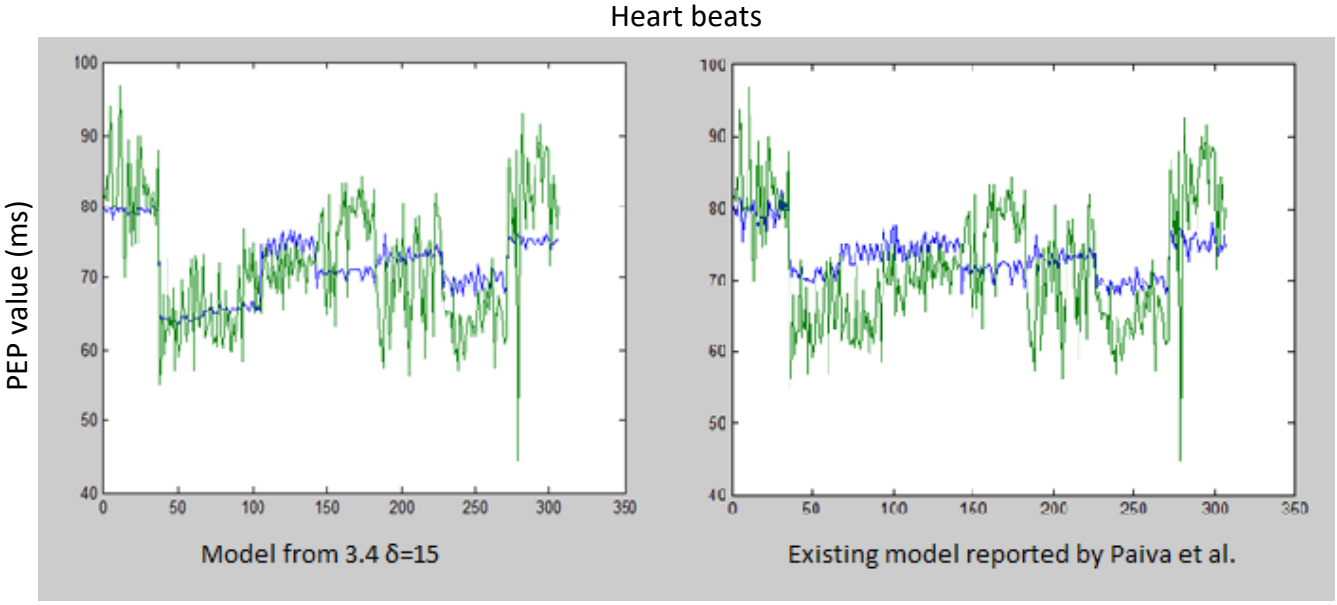


Figure 23 - Comparison of the results from the model described in 3.1.4 with the model proposed in 3.4.3, using δ= 15 ms (PEP(blue) and echo(green)).

This model provides results very similar with the model from Paiva et al [1]. The biggest difference between models in Figure 23 is represented between beats 50 and 100, where the extracted PEP values are closer to the ones from echo. This difference is reflected in the value of the error, decreasing slightly when using the new model. This suggests that the model implemented to extract PEP from PPG using LVET is a very promising tool regarding PEP extraction. To evaluate the statistical significance of the difference between the errors, a statistical analysis was applied. A Kolmogorov-Smirnov test was applied and since both distributions proved to be Gaussian a paired T-test was applied. With a $p - value = 5.3434 \times 10^{-21} < 0.01$ we can safely say that the differences are statistically significant. Therefore, considering the improvement of 12% in the error value, this model has a potential to assess PEP using PPG with high accuracy.

## 4.3 Other results

As it was mentioned previously, more procedures were performed for both multi-channel and single-channel approaches. This section is dedicated to the analysis of this results.

### 4.3.1 Multi-channel Audio-based Estimation of PEP from the best channel using PEP from the worst channel

For the multi-channel approach using a new probability distribution in the form of a Gaussian centered in the PEP value of the worst channel, we performed one more procedure where the standard deviation of this Gaussian was reduced to δ=15 ms. The main goal of this approach was to increase the influence of this Gaussian to assess PEP for best channel. The results can be observed in Table 18 and Table 19.

Table 18 - PEP median, mean and standard deviation results from Multi-channel audio based PEP extraction from best channel using PEP from the worst channel, in ms. δ=15.

| PEP estimation results (ms) | |
|---|---|
| Median | 71.0000 |
| Mean | 68.8877 |
| Standard deviation | 7.4011 |

Table 19 - PEP error mean and standard deviation results from Multi-channel audio based PEP extraction from best channel using PEP from the worst channel, in ms. δ=15.

| Error estimation results (ms) | |
|---|---|
| Mean | 10.0210 |
| Standard Deviation | 7.7412 |

The correlation value between PEP values extracted and PEP values from echo (golden standard) was 0.348 compared to the 0.418 obtained with a larger standard deviation.

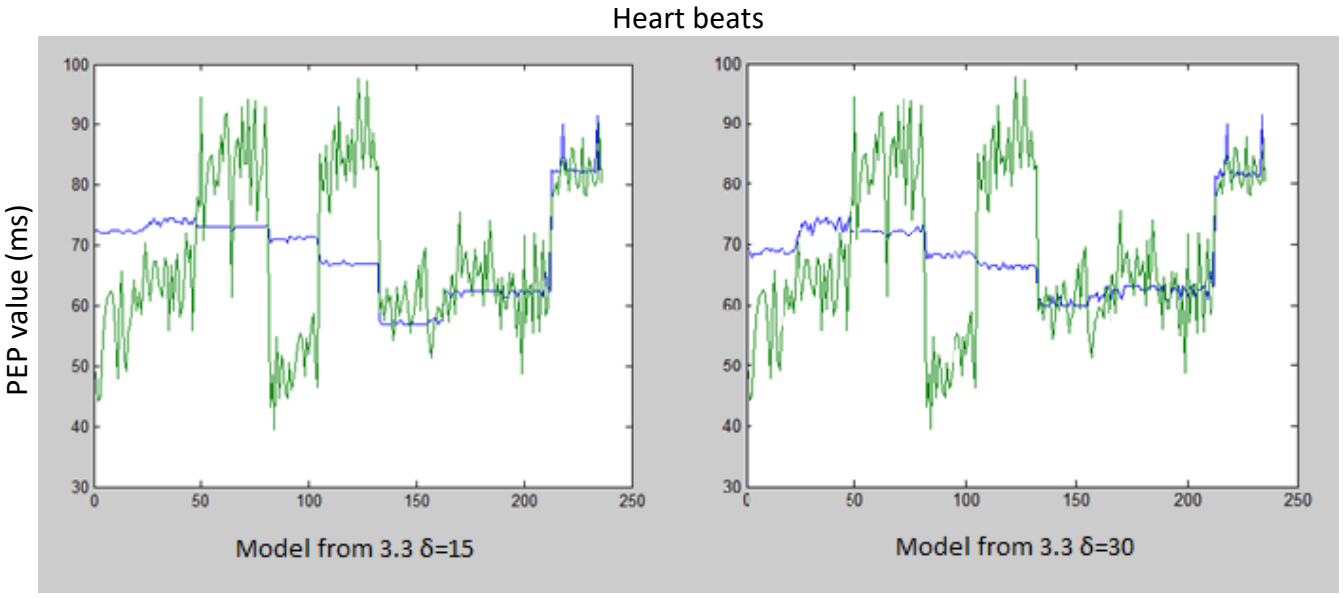


Figure 24 - Comparison of the results from the proposed model in 3.3 using δ= 15 ms and δ= 30 ms (PEP(blue) and echo(green)).

With the decrease of the standard deviation of the Gaussian centered in PEP from the worst channel, it is expected to see that Gaussian being to influence more the final result of PEP from ECG. With a major raise in the error of PEP calculation, it suggests that the information of PEP from the worst channel is not a good parameter to use to extract PEP from the best channel. Alongside the increase in the error value, the correlations suffered a major decrease corroborating the suspects.

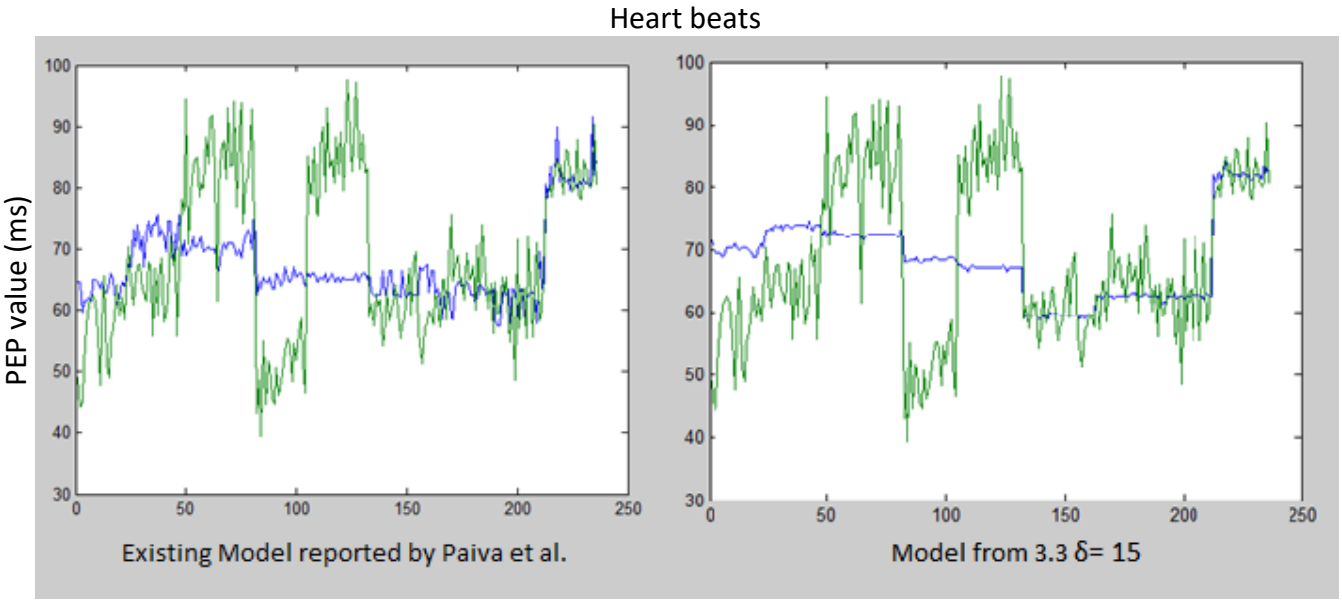


Figure 25 - Comparison of the results from the model described in 3.1.4 with the new model proposed (3.3) using δ= 15 ms (PEP(blue) and echo(green)).

As expected, when the δ= 15 ms the model results are worse than the ones extracted using the model reported by Paiva et al. [2]. The curve of extracted PEP values does not follow PEP values as good as the existing model does, suggesting one more time that using the PEP value from the worst channel is not a good procedure. Nevertheless, a statistical analysis was applied where a Kolmogorov-Smirnov test was proved both error distributions to be Gaussian and therefore a paired T-test was applied. Comparing the models, the results proved to be statistically significant with a $p - value = 3.2417 \times 10^{-7} < 0.01$.

### 4.3.2 Single-channel Audio-based Estimation of PEP using PPG: Model from 3.4.3

This section is dedicated to evaluate the results obtained with the model described in 3.4.3 with the standard deviation for the Gaussian used settled in 30 ms. The difference between the standard deviation is applied with the purpose of evaluating the influence of the new probability distribution extracted from PPG in the final extraction of PEP from heart sound.

Table 20 - PEP median, mean and standard deviation results from Single channel audio-based PEP estimation using PPG: model from 3.4.3, in ms. δ=30.

| **PEP estimation results (ms)** | |
|---|---|
| Median | 71.6667 |
| Mean | 72.3605 |
| Standard Deviation | 3.6508 |

Table 21 - PEP error mean and standard deviation results from Single channel audio-based PEP estimation using PPG: model from 3.4.3, in ms. δ=30

| **Error estimation results (ms)** | |
|---|---|
| Mean | 5.5633 |
| Standard Deviation | 4.1017 |

The correlation value between PEP values extracted and PEP values from echo (golden standard) was 0.645 compared to the 0.630 from the same model with a larger standard deviation.

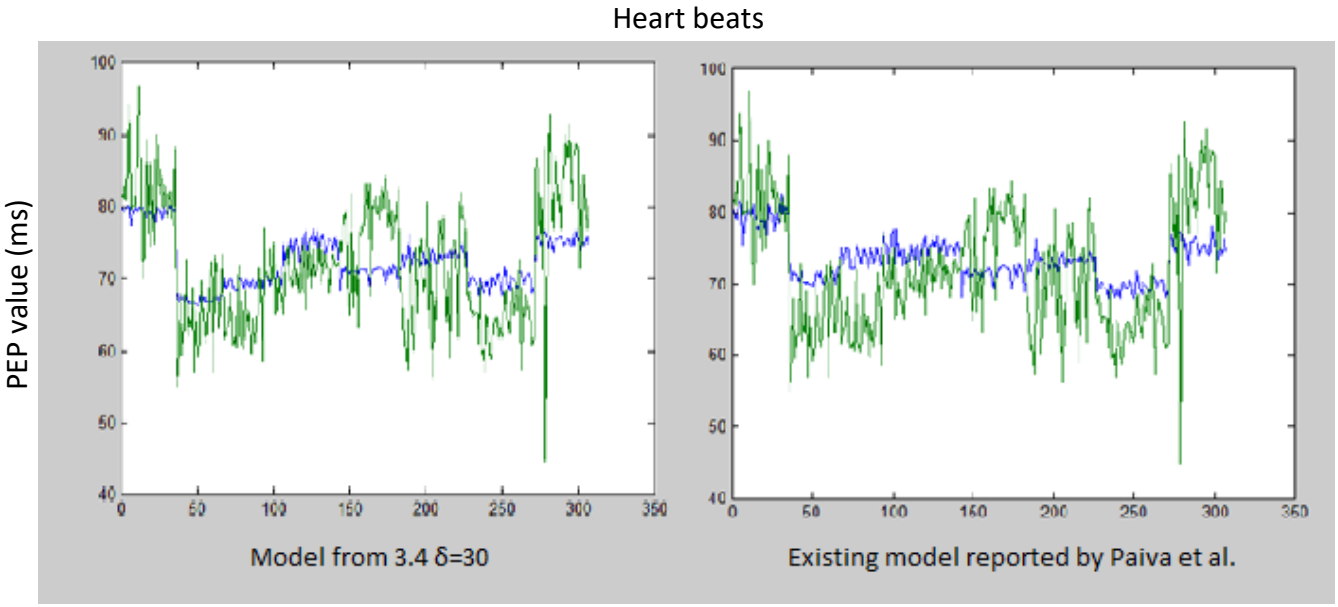


Figure 26 - Comparison of the results from the model described in 3.1.4 with the new model proposed (3.4.3) using δ= 30 ms (PEP(blue) and echo(green)).

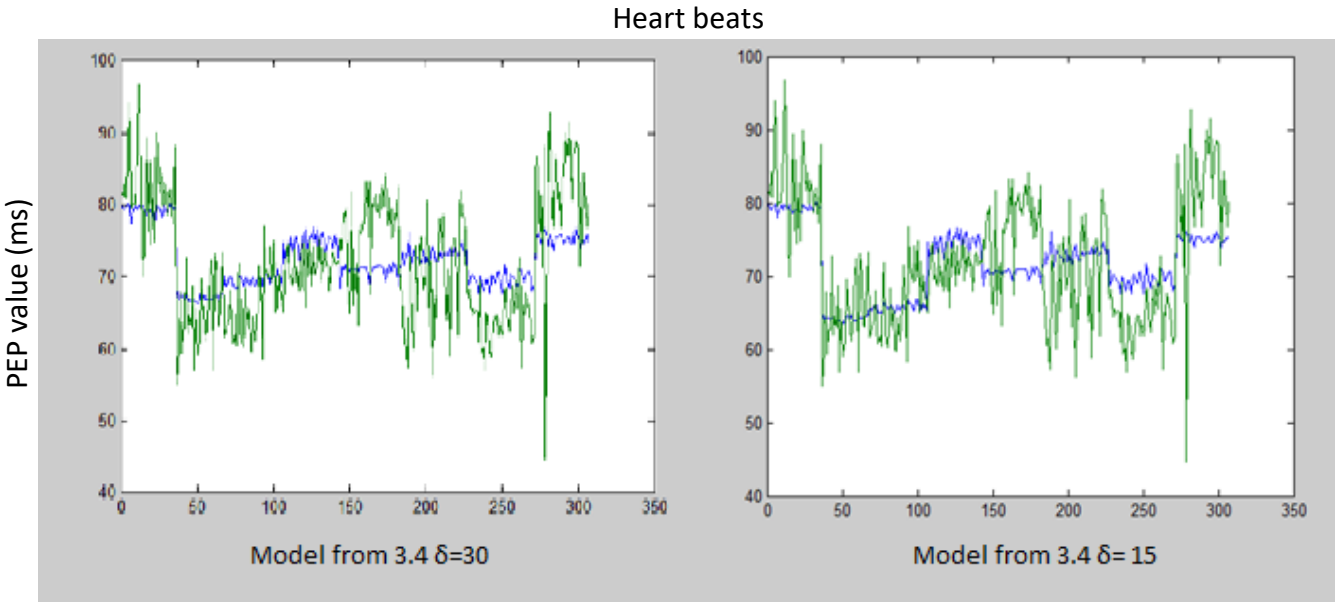


Figure 27 - Comparison of the results from the new model (3.4.3) using δ= 30 ms and δ= 15ms (PEP(blue) and echo(green)).

From Figure 27 it is possible to see that regardless the δ used, both procedures have very similar results, with the biggest difference being between beats 50 and 100. The error value is slightly higher when a larger standard deviation is used, which indicates that the probability distribution has a good effect in the accuracy of PEP extraction. With such similar results using two different values of

standard deviation, it is useful to verify is this difference is statistically significant. The Kolmogorov-Smirnov test proved both distributions to be Gaussian, and a paired T-test was applied. With a $p - value = 1.8143 \times 10^{-21} < 0.01$ the results proved to be statistically significant. The same procedure was applied between the results from this model and the model described in 3.1.4, and once again they proved to be statistically significant with a $p - value = 2.6868 \times 10^{-20} < 0.01$. The results strongly suggest that using this model is a good procedure, and the addition of the probability distribution of PEP value extracted from PEP improves the accuracy of the existing model.

### 4.3.3 Single-channel Audio-based Estimation of PEP using PPG: Model from 3.4.4

As described in section 3.4.4, a model without using PEP from the last heart beat was applied as well using PPG. This model was applied twice with standard deviation values δ=30 and δ=15. The first results shown are the ones regarding δ=30.

Table 22 - PEP median, mean and standard deviation results from Single channel audio-based PEP estimation using PPG: model from 3.4.4, in ms. δ=30.

| **PEP estimation results (ms)** | |
|---|---|
| Median | 71.3333 |
| Mean | 72.0065 |
| Standard Deviation | 4.1292 |

Table 23 - PEP error mean and standard deviation results from Single channel audio-based PEP estimation using PPG: model from 3.4.4, in ms. δ=30.

| **Error estimation results (ms)** | |
|---|---|
| Mean | 5.8685 |
| Standard Deviation | 4.5149 |

The correlation value between PEP values extracted and PEP values from echo (golden standard) was 0.522.

In the next two tables is possible to see the results from the same model, with a standard deviation δ=15 ms. As it was mentioned previously, the difference between the standard deviations is applied in order to evaluate the influence of the probability distribution in assessing PEP.

Table 24 - PEP median, mean and standard deviation results from Single channel audio-based PEP estimation using PPG: model from 3.4.4, in ms. δ=15

| **PEP estimation results (ms)** | |
|---|---|
| Median | 71.3333 |
| Mean | 71.5993 |
| Standard Deviation | 4.4824 |

Table 25 - PEP error mean and standard deviation results from Single channel audio-based PEP estimation using PPG: model from 3.4.4, in ms. δ=15

| **Error estimation results (ms)** | |
|---|---|
| Mean | 5.5935 |
| Standard Deviation | 4.3026 |

The correlation value between PEP values extracted and PEP values from echo (golden standard) was 0.586.

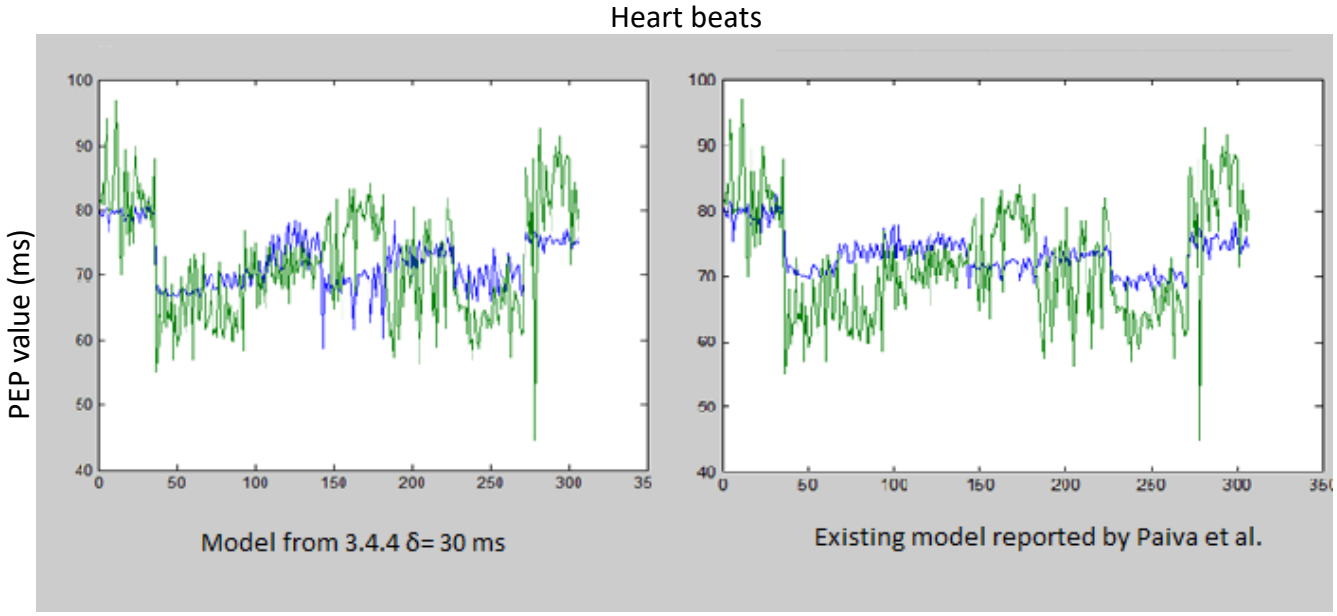


Figure 28 - Comparison of the results from the model described in 3.1.4 with the new model proposed (3.4.4) using δ= 30 ms (PEP(blue) and echo(green)).

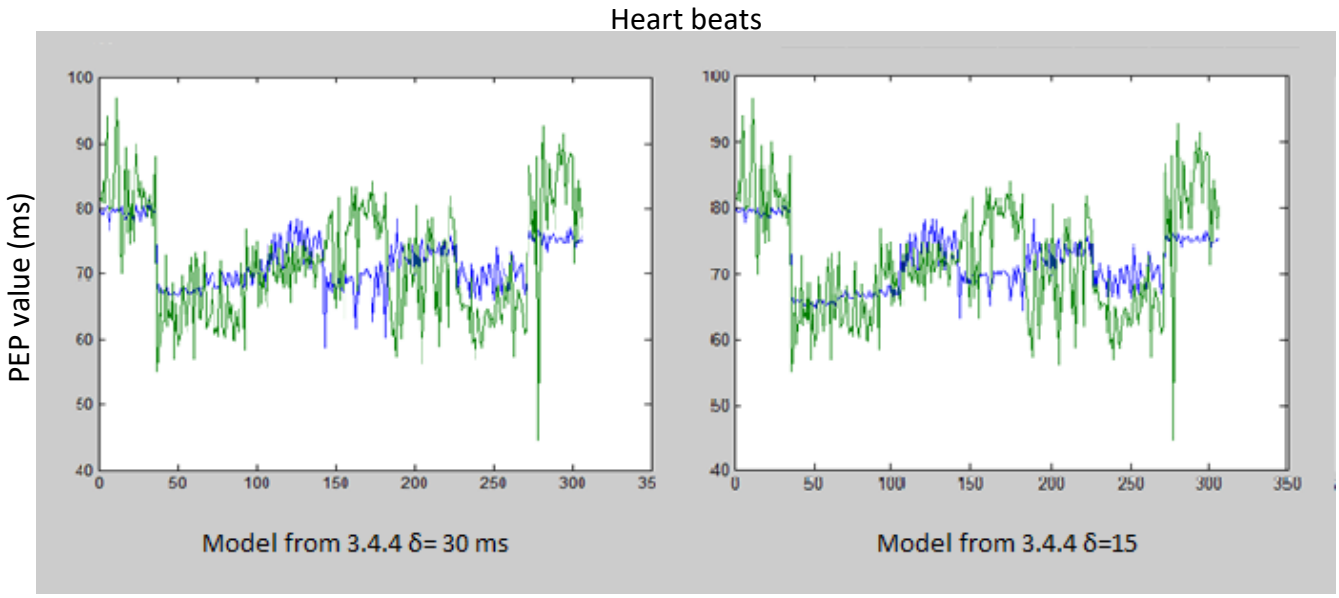


Figure 29 - Comparison of the results from the new model (3.4.4) using δ= 15 ms and δ= 30ms (PEP(blue) and echo(green)).

Once again the model proposed using PPG improves the accuracy in PEP extraction. The removal of $PEP_{k-1}$ is followed by a minor increase of the error in PEP from ECG calculation. Although the results are better than the results from the existing algorithm, showed in section 4.4, they are slightly worse

than the ones obtained while using PEP from the last beat. This result suggests that there is room to work in the model, and $PEP_{k-1}$ appear to not be absolutely necessary, which indicates that the model is performing well by not needing this limitation for PEP values. Nevertheless, it I possible to see that between beat 150 and 200 there's too much variation between PEP values of consecutive beast, which may be part of the cause of the decrease in the accuracy when compared to the method using $PEP_{k-1}$. A statistical analysis was applied to compare the results of this model with the one reported by Paiva et al. [1], and to compare the results between the different standard deviations inside the same model. All error distributions were proved to be Gaussian according to the Kolmogorov-Smirnov test, so paired T-tests were applied. All results have proved to be statistically significant, where the p-value between different standard deviations settled in 1.1830e-08. Between the new model using δ= 30ms and the existing model, $p - value = 1.9164 \times 10^{-26} < 0.01$ and when the standard deviation changed to δ= 15ms, the extracted $p - value = 1.3520 \times 10^{-24} < 0.01$.

# Chapter 5

# Conclusions

This thesis investigates two different possibilities to measure PEP using the HS. The first models developed study data from two different channels, and after the evaluation of each channel accuracy, they focus in the measure of PEP from the best channel, while using physiological properties from the worst channel. Since both channels contain data from the same patient, it is a good procedure to not discard information from any of those, even if the accuracy of the same is not as good as the other one. To this end, two different models were applied in order to use the information provided from both channel, to measure PEP values for the best channel. This study for the multi-channel approach was conducted on 8 healthy volunteers. Both models follow a Bayesian approach based in [1], where the channel selection was performed by a model reported in [2]. The second stage of this thesis is focused in a single channel model who aims to measure PEP in an audio-based approach, while using physiological properties acquired from a PPG signal.

For the multi-channel models created, the results obtained suggest that the new models represent a worse approach than the one reported by Paiva et al. [2]. Between the two models presented, it was not possible to verify an increase in the accuracy of measuring PEP when this information is used. This results might be related with the fact that the worst channel does not measure the physiological properties used with the same accuracy the best channel does. Nevertheless, the accuracy in measuring PEP does not decrease in a very significant scale, suggesting that both models have potential to be applied to extract PEP. Our results suggest that in a multi-channel approach it is better to not include information from channels that have worse performances based in the channel selection algorithm, and that information is not extracted with the necessary accuracy. Nevertheless, we find interesting the possibility of applying the model to a higher number of channels, representing an interesting study to perform in the future. The introduction of new channels represents an increase in the information that can be used to assess PEP that can be effective to improve the accuracy of this measurement.

To prove the statistical significance of these models, we would also like to extend the data collection as the current one is not very large. The main limitation of both models is the difficulty involved in the detection of the aortic valve opening, and a way to improve that can be using different signals to extract that timing, in an attempt to improve the performance of this procedure. In the future, we plan to extend this study to measure LVET as well.

After some approaches to achieve the multi-channel model, we realized that the acquisition and consequently the database might not be good enough. We were aware of this since the beginning, but we still though that it was worth to give it a try to improve the previous results. Data collection was changed to the one reported in [49] that was limited with data from only one channel. On the other hand, the new data collection was provided with information from a new signal, PPG. The initial goal of the second stage of this thesis was to segment S2 and study the split properties between its main components, but we decided to change the route and apply the Bayesian model reported in [1] to this data collection, in order to try to improve the existing model. To this end, we decided to use information from the new signal, PPG, by measuring PEP and creating a new probability distribution. PEP was calculated using LVET [49], S2start [1] and Q-peak [45] times as described previously. The results from the proposed models suggest the potential of the application of PPG when measuring PEP in an audio-based approach. This procedure provided an improvement in the accuracy of PEP measurement, by adding the information obtained from PPG. This supports the possibility that the accuracy in PEP measurement can be improved by using information from several signals. The larger the number of different signals, the larger will be the amount of information possible to extract, and the higher should be the accuracy in measuring physiological properties. In the future we want to extend the data collection in order to prove the statistical significance of this results. Also, we want to extend this study to measure LVET in an audio-based approach, while using LVET extracted from PPG to accurately measure the systolic time interval.

Bibliography

[1] R. P. Paiva, P. Carvalho, R. Couceiro, J. Henriques, M. Antunes, Muelsteff and J. Muehlsteff, "Beat-to-beat systolic time-interval measurement from heart sounds and ECG," *Physiological Measurement,* vol. 33, pp. 177-194, 2012.

[2] R. P. Paiva, T. Sapata, J. Henriques, I. Quintal, R. Baptista, L. Gonçalves and P. Carvalho., "Multi-channel audio-based estimation of the Pre-Ejection Period," in *2015 37th Annual International Conference of the IEEE Engineering in Medicine and Biology Society (EMBC)*, 2015.

[3] M. Nichols, N. Townsend, P. Scarborough and M. Rayner, "Cardiovascular disease in Europe 2014: epidemiological update," *European Heart Journal Advance Access,* vol. 35, no. 42, pp. 2950-2959, 2014.

[4] P.Carvalho, "Assessing cardiovascular function for pHealth applications," in *Gordon Research Conference on Advanced Health Informatics*, Hong-Kong, 2016.

[5] J. Forbes and R. T. H. Laennec, A Treatise on the Diseases of the Chest, and on Mediate Auscultation, New York,USA: Samuel S. and William Wood, 1838.

[6] D. Kumar, Automatic heart sound analysis for cardiovascular disease assesment (Unpublished doctoral thesis), Coimbra, Portugal, 2014.

[7] J. Oh and J. Tajik, "The Return of Cardiac Time Intervals," *Journal of the American College of Cardiology,* vol. 42, no. 8, pp. 1471-1474, 2003.

[8] W. F. Boron and E. L. Boulpaep, "The Cardiovascular System," in *Medical Physiology - A Cellular and Molecular Approach*, Philadelphia, Saunders(Elsevier), 2012, pp. 427-609.

[9] L. H. Opie and D. M. Bers, "Mechanisms of Cardiac Contraction and Relaxation," in *Braunwald's Heart Disease: A Textbook of Cardiovascular Medicine Tenth Edition*, Philadelphia, Saunders(Elsevier ), 2015, pp. 21,429-453.

[10] E. G. Dimond and A. Benchimol, "Phonocardiography," *Calif. Med.,* vol. 94, no. 3, p. 139–146, 1961.

[11] Z. Fei and L. Yong, "QRS Detection Based on Multiscale Mathematical Morphology for Wearable ECG Devices in Body Area Networks," *IEEE Transactions on Biomedical Circuits and Systems,* vol. 3, no. 4, pp. 220-228, 2009.

[12] C. F. Zhang and T.-W. Bae, "VLSI Friendly ECG QRS Complex Detector for Body Sensor Networks," *IEEE Journal on Emerging and Selected Topics in Circuits and Systems,* vol. 2, no. 1, pp. 52-59, 2012.

[13] R. M. Berne and M. N. Levy, Cardiovascular Physiology: Mosby Physiology Monograph Series, St. Louise: Mosby, 1997.

[14] M. Young-Jae, K. Hoon-Ki, K. Yu-Ri, K. Gil-Su, P. Jongsun and K. Soo-Won, "Design of Wavelet-Based ECG Detector for Implantable Cardiac Pacemakers," *IEEE Transactions on Biomedical Circuits and Systems,* vol. 7, no. 4, pp. 426-436, 22013.

[15] J. Allen, "Photoplethysmography and its application in clinical physiological measurement," *Physiological Measurement,* vol. 28, no. 3, pp. R1-R39, 2007.

[16] R. Gonzalez, A. Manzo, J. Delgado, J. Gomis-Tena and J. Saiz, "Photoplethysmographic Augmentation Index Using the Signal Fourth Derivative," in *IEEE Conference Publications, Computing in Cardiology*, Krakow, 2012.

[17] M. Alnaeb, N. Alobaid, A. Seifalian, D. Mikhailidis and G. Hamilton, "Optical Techniques in the Assessment of Peripheral Arterial Disease," *Current Vascular Pharmacology,* vol. 5, no. 1, pp. 53-59, 2007.

[18] D. Lemonick, "Evaluation of Syncope in the Emergency Department," *American Journal of Clinical Medicin,* vol. 7, no. 1, pp. 11-19, 2010.

[19] C. Ahlstrom, P. Hult and P. Ask, "Detection of the 3rd Heart Sound Using Recurrence Time Statistics," in *IEEE International Conference on Acoustics, Speech and Signal Processing*, 2006.

[20] H. Abe, M. Yokouchi, F. Deguchi, F. Saitoh, H. Yoshimi, Y. Arakaki, T. Natsume, Y. Kawano, K. Yoshida, M. Kuramochi and e. al., "Measurement of left atrial systolic time intervals in hypertensive patients using Doppler echocardiography: relation to fourth heart sound and left

ventricular wall thickness.," *Journal of the American College Cardiology,* vol. 11, no. 4, pp. 800-805, 1988.

[21] D. Sapire, Understanding and diagnosing pediatric heart disease: Heart sounds and mur-murs, Norwalk, Connecticut: Applcton & Lange, 1992.

[22] J. Wartak, Phonocardiology; integrated study of heart sounds and murmurs, New York: Harper & Row, 1972.

[23] T. M, Clinical Phonocardiography and External Pulse Recording, Chicago: Year Book Medical Publishers, 1967.

[24] D. Cokkinos, E. Heimonas, J. Demopoulos, A. Haralambakis, G.Tsartsalis and C. Gardikas, "Influence of heart rate increase on uncorrected pre-ejection period/left ventricular ejection time (PEP/LVET) ratio in normal individuals," *British Heart Journal,* vol. 38, no. 7, pp. 683-688, 1976.

[25] J. Muehlsteff, X. Aubert and M. Schuett, "Cuffless estimation of systolic blood pressure for short effort bicycle tests: the prominent role of the pre-ejection period," in *Int. Conf. of the IEEE Engineering in Medicine and Biology Society*, 2006.

[26] S. Finckelstein and J. Cohn, "Method and apparatus for measuring cardiac output". United States of America Patent 5241966, 7 September 1993.

[27] J. Davis, "The physiology of congestive heart failure," in *Handbook of physiology*, Washington DC, American Physiological Society, 1965, p. 2071–2122.

[28] S. Hassan and P. Turner, "Systolic time intervals: a review of the method in the non-invasive investigation of cardiac function in health, disease and clinical pharmacology," *Postgraduate Medical Journal,* vol. 59, pp. 423-434, 1983.

[29] J.-L. Vincent, "Understanding cardiac output," *Critical Care,* vol. 12, no. 4, p. 174, 2008.

[30] R. P. Lewis, S. E. Rittogers, W. F. Froester and H. Boudoulas, "A critical review of the systolic time intervals.," *Circulation,* vol. 56, pp. 146-158, 1977.

[31] A. M. Weissler, W. S. Harris and Clyde D. Schoenfeld, "Systolic time intervals in heart failure in man.," *Circulation,* vol. 37, no. 2, pp. 149-159, 1968.

[32] K. L. Wanderman, Z. Hayek, I. Ovsyshcher, G. Loutaty, A. Cantor, Y. Gussarsky and M. Gueron, "Systolic Time Intervals in Adolescents Normal Standards for Clinical Use and Comparison with Children and Adults," *Circulation,* vol. 63, no. 1, pp. 204-209, 1981.

[33] F. V. d. Werf, J. Piessens, H. Kesteloot and H. D. Geest, "A comparison of systolic time intervals derived from the central aortic pressure and from the external carotid pulse tracing," *Circulation,* vol. 51, no. 2, pp. 310-316, 1975.

[34] P. Carvalho, R. P. Paiva, R. Couceiro, J. Henriques, M. Antunes, I. Quintal, J. Muehlsteff and X. Aubert, "Comparison of Systolic Time Interval Measurement Modalities for Portable Devices," in *32nd Annual International Conference of the IEEE EMBS*, Buenos Aires, 2010.

[35] W. Harris, C. Schoenfeld and A. Weissler, "Effects of adrenergic receptors activation and blockade on the systolic preejection period, heart rate and arterial pressure in man.," *Journal of Clinical Investigation,* vol. 46, no. 11, p. 1704, 1967.

[36] A. Q. Javaid, H. Ashouri and O. T. Inan, "Estimating Systolic Time Intervals During Walking Using Wearable Ballistocardiography," in *IEEE-EMBS International Conference on Biomedical and Health Informatics*, 2016.

[37] H. Luo and Z. Wang, "Algorithms Development for Systolic Time Intervals and Clinical Assessment of Cardiac Function," in *Proceedings of the 22nd Annual EMBS International Conference*, Chicago, 2000.

[38] A. Q. Javaid, N. F. Fesmire, M. A. Weitnauer and O. T. Inan, "Towards Robust Estimation of Systolic Time Intervals Using Head-to-Foot and Dorso-Ventral Components of Sternal Acceleration Signals," in *IEEE 12th International Conference on Wearable and Implantable Body Sensor Networks (BSN)*, 2015.

[39] P. Carvalho, R. P. Paiva, R. Couceiro, J. Henriques, I. Quintal, J. Muehlsteff, X. L. Aubert and M. Antunes, "Assessing Systolic Time-Intervals from Heart Sound: A Feasibility Study," in *31st Annual International Conference of the IEEE EMBS*, Minneapolis, Minnesota, USA, 2009.

[40] T. Onu, M. Miyamura, Y. Yasuda, T. Ito, T. Saito, T. Ishiguro, M. Yoshizawa and T. Yambe, "Beat-to-beat evaluation of systolic time intervals during bicycle exercise using impedance," *Tohoku J Exp Med,* vol. 203, no. 1, pp. 17-29, 2004.

[41] P. Carvalho, R. P. Paiva, J. Henriques, M. Antunes, I. Quintal and J.Muehlsteff, "Impedance Cardiogram: evaluation of existing and new characteristic point definitions," *(under preparation).*

[42] R. Paiva, P. Carvalho, J. Henriques, M. Antunes, J. Muehlsteff and X. Aubert, "Assessing PEP and LVET from Heart Sounds: Algorithms and Evaluation," in *Int. Conf. of the IEEE Engineering in Medicine and Biology Society*, 2009.

[43] G. Chan, P. Middleton, B. Celler, L. Wang and N. Lovell, "Automatic detection of left ventricular ejection time from a finger Photoplethysmography pulse oximetry waveform: comparison with Doppler aortic measurement," *Physiological Measurement,* vol. 28, no. 4, pp. 439-452, 2007.

[44] D.-N. Jiang, L. Lu, H.-J. Zhang, J.-H. Tao and L.-H. Cai, "Music type classification by spectral contrast feature," in *IEEE International Conference on Multimedia and Expo*, 2002.

[45] J. Henriques, P. Carvalho, M. Harris, M. Antunes, R. Couceiro, M. Brito and R. Schmidt, "Assessment of Arrhythmias for Heart Failure Management," in *phealth2008 - International Workshop on Wearable Micro and Nanosystems for Personalised Health*, 2008.

[46] R. P. Paiva, T. Mendes and A. Cardoso, "From Pitches to Notes: Creation and Segmentation of Pitch Tracks for Melody Detection in Polyphonic Audio," *Journal of New Music Research,* vol. 37, no. 3, pp. 185-205, 2008.

[47] W. SJ, W. K and B. CD., "Correction of systolic time intervals for heart rate: a comparison of individual with population derived regression equations," *British Journal of Clinical Pharmacology,* vol. 26, no. 2, pp. 155-165, 1988.

[48] R. Couceiro, P. Carvalho, R. P. Paiva, J. Henriques, I. Quintal, M. Antunes, J. Muehlsteff, C. Eickholt, C. Brinkmeyer, M. Kelm and C. Meyer, "Assessment of cardiovascular function from multi-Gaussian fitting of a finger photoplethysmogram," *Physiological Measurement,* vol. 36, no. 9, pp. 1801-1825, 2015.

[49] R. Couceiro, P. Carvalho, R. P. Paiva, J. Henriques, M. Antunes, I. Quintal and J. Muehlsteff, "Multi-Gaussian fitting for the assessment of left ventricular ejection time from the Photoplethysmogram," in *2012 Annual International Conference of the IEEE Engineering in Medicine and Biology Society*, 2012.